Title

CHEMISTRY AND MORPHOLOGY OF COAL LIQUE- VACTION. SECOND QUARTERLY SUMMARY REPORT. JANUARY 1 - MARCH 31, 1980

Author

Heinemann, Heinz.

Publication Date

1980-03-01

Lawrence Berkeley Laboratory
UNIVERSITY OF CALIFORNIA

Materials & Molecular Research Division

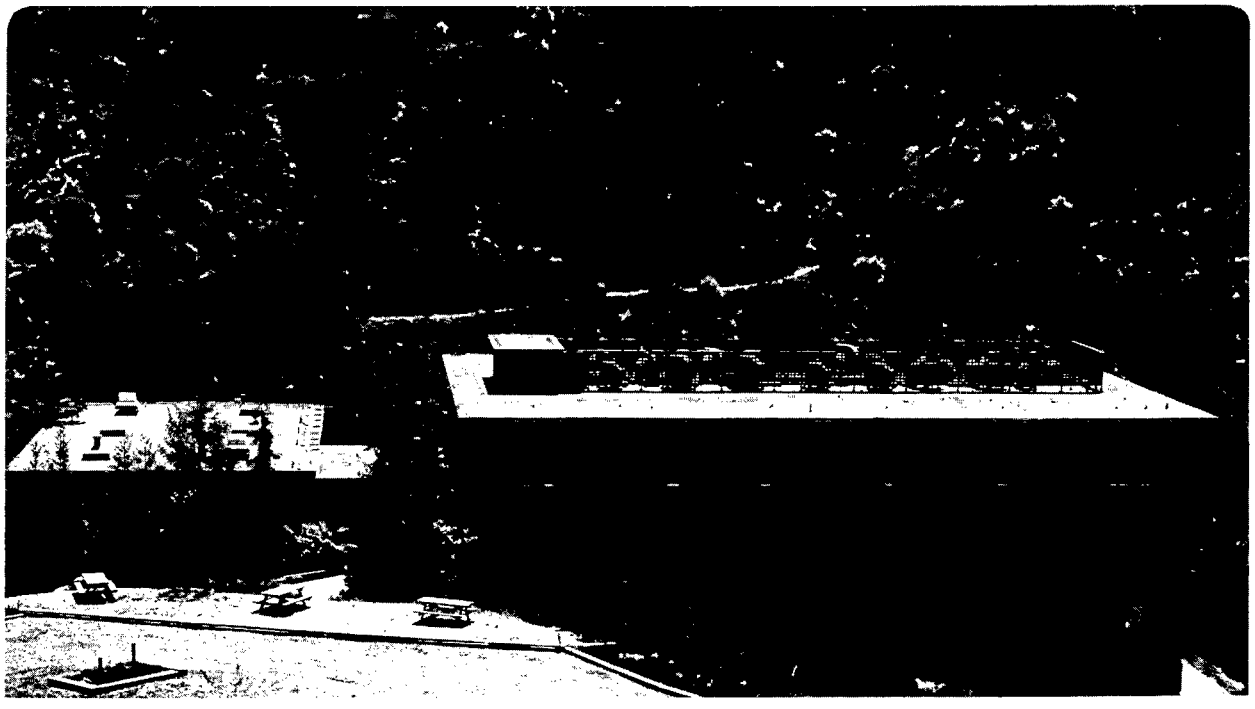

DISCLAIMER

SECOND QUARTERLY SUMMARY REPORT

January 1 - March 31, 1980

CHEMISTRY AND MORPHOLOGY OF COAL LIQUEFACTION

Contract ET-78-G-01-3425

Principal Investigator: Heinz Heinemann
Lawrence Berkeley Laboratory, Bldg. 62
University of California
Berkeley, CA 94720

Task 1: Selective Synthesis of Gasoline Range Compounds from Synthesis Gas. Task Manager: A. T. Bell

Since the last report, efforts have focused on the design and construction of experimental apparatus. To date a high pressure gas manifold and fixed reactor have been designed and the necessary components ordered. Assembly of this unit will begin in the next few weeks. Once completed this apparatus will be used to evaluate iron and ruthenium catalysts prepared on different supports. An apparatus to be used for the study of mass transfer effects is also being designed at present. Originally it was planned to use a design in which a thin film of liquid is flowed over a flat plate which comprises the catalyst. This configuration has now been dropped because calculations have shown that it would be quite difficult to operate a reactor using the initially proposed approach. Instead we have decided to use porous catalyst pellets contained in a rotating basket. This design represents a modification of the Berty reactor and has been used successfully at Amoco. Our plan is to construct such a reactor using a small Paar autoclave. Modifications will be made to a small Paar autoclave to accommodate the spinning basket and to provide for a continual supply and removal of a liquid phase. The liquid will serve to improve heat transfer from the catalyst and will help remove heavy products from

contact with the catalyst. The autoclave and parts for a flow manifold have been ordered and assembly of the apparatus will begin once components are received.

Task 2: Cancelled

Task 3: Electron Microscope Studies of Coal During Hydrogenation, Task Manager: J. W. Evans, with J. A. Little and K. H. Westmacott

The liquefaction and gasification of various coals are increasingly important technological utilizations of coal which are dependent upon its physical characteristics as well as its chemistry. In this respect, both the size and distribution of pores and the size, distribution and chemical identity of the submicron size minerals are physical parameters of great interest because of their probable influence in the coal conversion processes. In Berkeley, this study is proceeding by examination of such processes using an environmental cell in a high voltage microscope, by which the influence of different gases, temperatures and pressure upon the gasification reaction can be studied. An important first step in such a study is the primary characterization of the coals to be studied and the combined use of both transmission (TEM) and scanning transmission electron microscope (STEM) analyses utilizing both convergent beam methods and an energy dispersive X-ray analytical detector is thus a powerful tool in such a characterization.

Many varied coal types will be examined and here we present some results of the examination of both high- and low-ash anthracites and a high volatile class A bituminous coal (Vitrinite). Specimens were prepared by a careful mechanical grinding using silicon carbide and diamond pastes, followed by conventional ion-beam thinning. A Phillips 400 TEM/STEM electron microscope was used for the investigation.

Figure 1 shows a low-ash anthracite and an example of the mineral matter it contains. A small probe size (≃20nm) was used to obtain convergent beam patterns, an example of which is shown. Thus the particle was indexed as hexagonal with a c/a ratio of approximately 1.6. The X-ray spectrum from the particle as compared with an adjacent area show an almost pure titanium peak and thus the particle was identified at Ti_2O.

In Figure 2 a high-ash anthracite (≃40%) can be seen with some associated phenomena. The particle at A is again a mineral containing merely titanium although micro-diffraction patterns were not taken to establish the exact nature of the mineral. At B a crystalline area can be seen and the inset diffraction pattern shows a typical diffraction pattern obtained from such an area. The extensive streaking indicates a crystalline area composed of thin crystal platelets perpendicular to the streaks. The exact nature of these thin areas has not yet been determined but EDX has shown them to contain high concentrations of both potassium and iron. The difficulty in such determination is that on exposure to the electron beam this area transforms to that at C (and has already done so to some extent in this example, the diffraction pattern thus indicating the initial conditions) which then shows a typical amorphous diffraction pattern. High voltage microscopy is being undertaken to ascertain whether this effect is due to beam heating or ionization damage.

Figure 3 shows features from the bituminous coal (Vitrinite). Both large-scale and small-scale porosity can be seen in a) and b) as well as the banding effect in c) commonly seen in lower magnification optical microscopy of these coals. These micrographs are all from the same specimen and microstructural differences seen do reveal differences in the coal over very small distances. However, the absolute microstructure itself may be influenced by preparation techniques and beam heating in the

ion-miller, and has still to be investigated. The typical diffraction pattern shows diffuse rings corresponding to d-spacings of from 4.3A to 5A in agreement with previous X-ray work on such coals (1).

(1) Ergun, S. and Tiensuv, V., Nature (1959) 183, p. 1669.

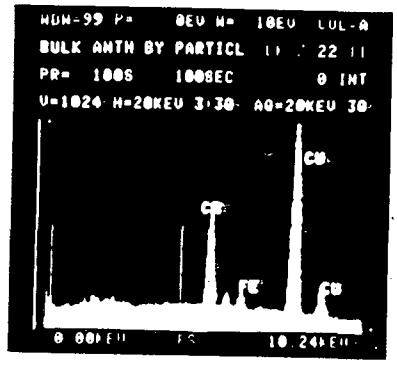

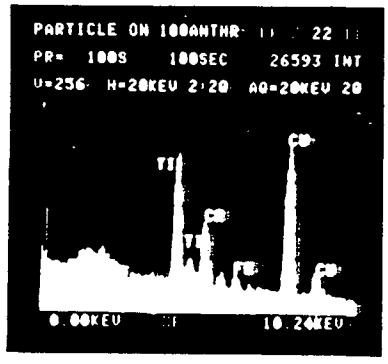

Fig. 1 (above) Low ash anthracite showing convergent beam pattern of titania inclusion. (right) EDX analyses of particle and surrounding material.

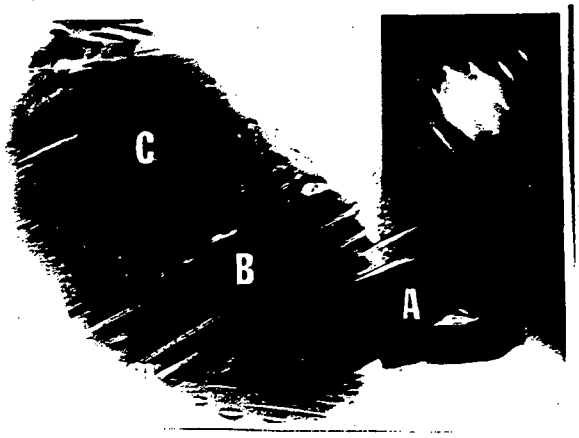

Fig. 2 (left) High-ash anthracite showing mineral matter and micro-crystallinity.

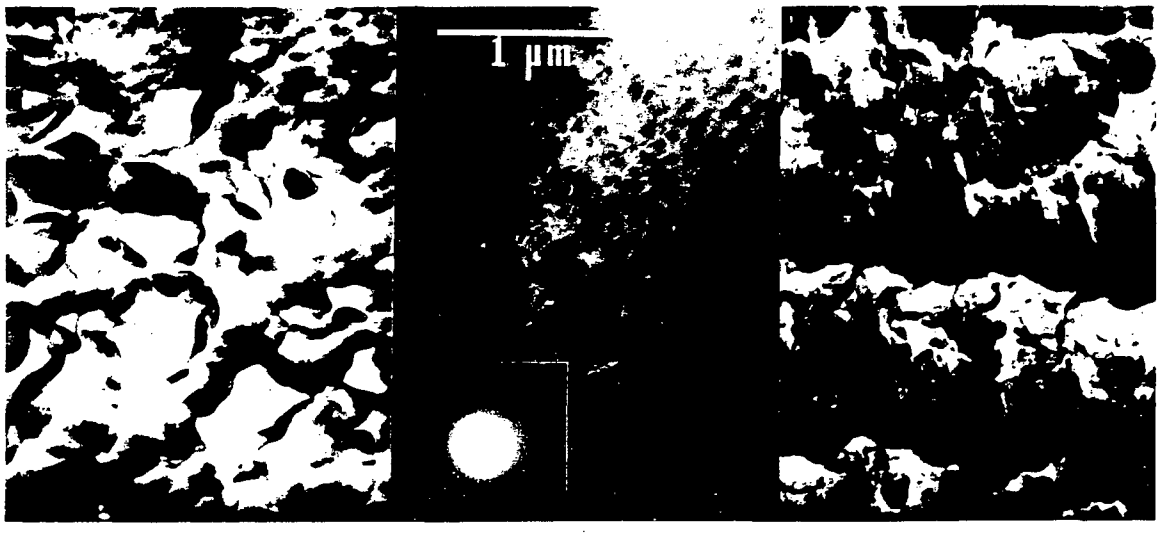

Fig. 3 High volatile Calss A bituminous coal (Vitrinite) showing porosity and "banding."

Task 4: Catalysed Low Temperature Hydrogenation of Coal
Task Manager: G. A. Somorjai

The high pressure apparatus shown in photos attached to the previous report is almost completed. It is assembled and, with the exception of the oil diffusion pump, all the parts are in place. The electronic instrumentation, however is yet to be installed. The double pass cylindrical mirror analyzer that is to be used for Auger electron spectroscopy and photo-electron spectroscopy has not been delivered as yet, and the ion bombardment gun and gas chromatograph have not been received. These should appear during the next two weeks.

Dr. Alejandro Cabrera, a new posdoctoral fellow, has been hired from the San Diego campus. He has visited the laboratory and he is to start employment on May 1. It is clear that he should be running the first experiments during the early part of June. In view of the complexity of the equipment being installed, this is a very satisfactory schedule.

Task 5: Selective Hydrogenation, Hydrogenolysis and Alkylation of Coal and Coal Liquids by Organo Metallic Systems. Task Manager: K.P.C. Vollhardt.

The feasibility of using a cyclopentadienyl-cobaltbenzene dication complex as a model system for the potential transition metal mediated alkylation of coal molecules has been further explored. So far the only reaction that seems to be working is the reaction with methanol which introduces two methoxide substituents into the benzene ring. However, the resulting complex is exceedingly air sensitive and thermally unstable. Decomposition results in polymer formation and no defined organic product can be obtained. Reaction of the benzene dication with a variety of other potential nucleophiles has not led to characterizable products.

The potential of stepwise alkylation via successive hydride abstraction-nucleophilic attack processes was briefly examined but did not provide any significant improvement in product yields and scope. Thus, it appears that although a potentially highly significant and novel reaction has been discovered, its limitations are severe at least as far as the unsubstituted benzene ligand is concerned. Work is currently being extended to other metals, and in particular, to other ligands. The latter will involve more extended π-systems of the anthracene and phenanthrene type. The former will involve iron and manganese complexed aromatic systems which might show improved stability but maintain the same reactivity patterns as the cobalt system.

Task 6: Chemistry of Coal Solubilization and Liquefaction. Pyrolysis Studies. Task Manager: R. G. Bergman

A paper on "Flow Pyrolysis and Direct and SiF_4-sensitized Laser Induced Decomposition of Tetralin" is attached. Additional work is summarized in the following:

We have recently prepared and examined the pyrolysis of compounds 1 and 2 in the gas phase and in solution. Equilibration of 1 and 2 is rapid with respect to intramolecular hydrogen atom transfer and strongly favors diacetylene 2. At higher temperatures, the gas phase pyrolysis of 1 or 2 produces tetralin and o-ethylstyrene. The slow intramolecular trapping of 1,4-dehydrobenzene 3 contrasts sharply with the 2,3-dipropyl substituted 1,4-dehydrobenzene we examined previously. This difference in reactivity must reflect the kinetic preference for a six versus five-membered transition state in intramolecular hydrogen transfer (the thermodynamics of reaction in the diethyl and dipropyl 1,4-dehydrobenzenes are expected to be virtually identical).

When compound 1 is pyrolyzed in benzene solution at 190°C, 2 is the major product. There is observed, however, a small yield (5%) of o-diethylbenzene and a small amount of bibenzyl. Observation of these products suggests that the 1,4-dehydrobenzene direadical is capable of abstracting hydrogen from the benzene solvent. By this argument, bibenzyl results from the random combination of phenyl radicals. Addition of 10% 1,4-cyclohexadiene to the benzene solution of 1 diverts the products of pyrolysis almost exclusively to o-diethylbenzene; intermolecular trapping of 3 is some 15 times faster than rearrangement to 2.

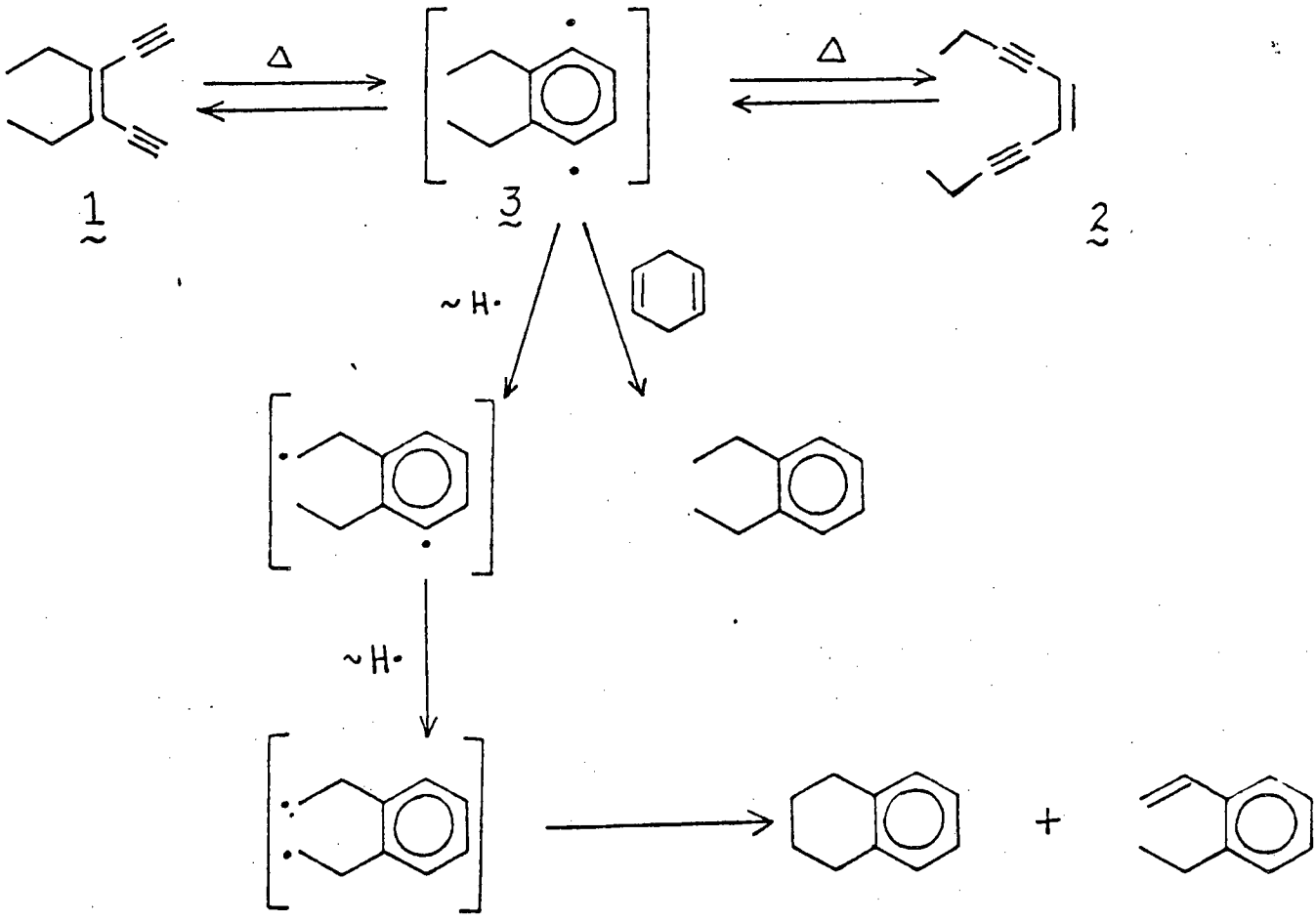

Task 7: Coal Conversion Catalysts-Deactivation Studies.
Task Managers: A. V. Levy and E. E. Petersen

The report mentioned in the Jan 15, 1980, letter is attached. This work was done prior to the present program's initiation. A post-doctoral has been hired to carry out the controlled aging experiments and he has designed equipment, which is currently being manufactured. In the meantime, porosity studies are being undertaken on the commercially aged catalyst samples on hand.

This work was supported by the U.S. Department of Energy under Contract number W-7405-ENG-48.

Flow Pyrolysis and Direct and SiF_4-Sensitized Laser-Induced Decomposition of Tetralin. Identification of Retro-[2+4] Cleavage as the Primary Homogeneous Thermal Decomposition Channel

By Michael R. Berman, Paul B. Comita,
C. Bradley Moore and Robert G. Bergman
Lawrence Berkeley Laboratory, University of California, Berkeley, CA94720

Abstract

In an effort to determine the products and mechanism of the truly homogeneous thermal decomposition of the aromatic hydrocarbon tetralin, we have examined the products formed from this compound upon energization by conventional flow pyrolysis, infrared multiphoton excitation, and SiF_4-sensitized infrared laser thermal activation. Six major products are formed in these reactions, but the product ratios depend upon the mode of energization. Flow pyrolysis gives a result analogous to those observed earlier; i.e., almost exclusive dehydrogenation, leading to dihydronaphthalene and napthalene. Direct and sensitized IR laser-induced decomposition, however, leads to ethylene loss (presumably by an initial retro-[2+4] reaction) as the predominant decomposition mode, giving benzocyclobutene. We believe these results are due to the fact that direct thermal decomposition, both in our experiments as well as in previous studies, involves predominant surface-catalysis. In the laser-induced reactions, which are uncomplicated by problems due to surface-catalysis, the true homogeneous decomposition takes place, and this involves retro-[2+4] cleavage. Mechanistic details of these processes were studied by examining the isotope distribution in the products formed on SiF_4-sensitized laser photolysis of 1,1,4,4-tetradeuteriotetralin.

Flow Pyrolysis and Direct and SiF_4-Sensitized Laser-Induced Decomposition of Tetralin. Identification of Retro-[2+4] Cleavage as the Primary Homogeneous Thermal Decomposition Channel.

Sir:

The thermal chemistry of tetralin (1) has been under intense investigation recently[1], due to interest in the fate of hydrogen donors which are used as recycle liquids in the solvent refining of coal. The reactivity of tetralin appears to be dependent on the presence of hydrogen, hydrogen acceptor molecules, different types of reactor surfaces, and surface history. This has resulted in conflicting data[2] in the literature and confusion as to what the thermal reactivity is in the absence of any catalytic effects. In an effort to resolve this situation, we wish to report the reactivity of tetralin resulting from several different methods of activation.

Three methods for energization of 1 were investigated: conventional flow pyrolysis, infrared multiphoton excitation, and sensitized infrared laser thermal activation. All three give rise to six major products: benzocyclobutene (2), styrene (3), o-allyltoluene (4), indene (5), 1,2-dihydronaphthalene (6), and naphthalene (7) (see Scheme 1), and several minor products[3]. The primary concern of this work is to delineate the energetics of the ethylene-loss channel (giving rise to 2 and 3) versus the hydrogen-loss channel (giving rise to 6 and 7) without

interference from catalytic effects.

A number of parameters affected the product distribution for the decomposition in a flow reactor[4], including the composition of the surface, the history of the surface, and the pressure of the system (see Table 1). However, dehydrogenation was always the predominant decomposition mode. Unconditioned surfaces, higher pressures, and longer contact times in the reactor led to more dehydrogenation of **1**.

Multiphoton excitation of **1** in the gas phase was accomplished[5] with a pulsed CO_2 TEA laser[6,7] tuned to 945.99 cm^{-1}. All six major products[8] found from the pyrolysis also resulted from photolysis of tetralin, including one additional product, phenylacetylene[9]. The distribution of these products, however, was at variance with the distribution from the pyrolysis (see Table 1); the major reaction channel for the multiphoton dissociation of tetralin involved ethylene loss.

In the third method of activation, **1** and varying pressures of SiF_4, an inert sensitizer[10] which absorbs strongly in the infrared, were irradiated[11] with an unfocused, pulsed CO_2 TEA laser tuned to 1027.36 cm^{-1}. Pure tetralin does not decompose under unfocused conditions; thus all chemistry is due to sensitization by SiF_4. All six major products were again found.

The number of pulses and the maximum temperature[12] of SiF_4 both had pronounced effects on the product distribution. The variation in the number of pulses had a number of effects. With increasing number of pulses the percentage of **2** and **6** decreased, and the percentage of **3**, **5**, and **7** increased. This is

consistent with 2 and 6 being primary products, and at least some fraction of 3, 5, and 7 being derived from them. Sensitized photolysis[13] of 2 gave rise to a clean isomerization to 3, the sole product of the reaction (70% conversion). Sensitized photolysis[13] of 6 (20% conversion) gave rise to two major products[14], 7 (68% of product) and 5 (11%).

Temperature variation was achieved by changing the beam intensity and by varying the sensitizer pressure. Less secondary decomposition took place at lower temperatures, and there was a partitioning between the retro-[2+4] channel and the dehydrogenation channel (see Table 1). The ethylene-loss channel increased relative to dehydrogenation as the temperature was lowered, consistent with it being the low energy reaction channel for tetralin.

In order to further elucidate the mechanism of reaction of tetralin, 1,1,4,4-tetradeuteriotetralin ($1\text{-}d_4$) was synthesized[15] and subjected to sensitized photolysis. The labeling results[16] indicate that the retro-[2+4] product results entirely from C_2H_4 loss and the dehydrogenation <u>is predominantly a result of 1,2-elimination</u> (see Table 2).

Since thermal 1,2-elimination of hydrogen is unusual[17], the nature of this reaction is of interest. The surface to volume ratio[18] for the photolysis cell had no effect on the ratio of ethylene-loss/dehydrogenation for the sensitized photolysis. The possibility of a radical chain mechanism for the dehydrogenation was tested for by charging the photolysis cell with 1 Torr of

nitric oxide. The only observed effect of nitric oxide was to lower the effective temperature for the photolysis. A decrease in the partial pressure of tetralin from 0.325 Torr to 0.032 Torr also had no effect on the ratio of ethylene-loss to dehydrogenation.

We draw the following conclusions from the above experiments: (1) Some fraction of the dehydrogenation reaction in the flow reactor is surface catalyzed. This leads to an anomalously large amount of 1,2-dihydronaphthalene and naphthalene in the reaction products in these flow pyrolysis studies and very likely in all previous investigations. (2) The lowest energy homogeneous reaction channel for tetralin is the retro-[2+4] channel giving rise to benzocyclobutene. This fact is borne out in both the multiphoton and SiF_4 sensitized experiments where surface chemistry does not appear to be important. (3) The low energy dehydrogenation channel of tetralin is almost exclusively 1,2-dehydrogenation. This process, if concerted, is symmetry forbidden and without precedent as the lowest energy dehydrogenation channel in cyclic olefins. Evidence for a radical pathway by radical scavenging experiments was not found. Bimolecular pathways for this process were also not detectable by changing the partial pressure of 1.

The reactivity of tetralin contrasts with that of its olefinic analog cyclohexene[17] in a number of ways. The rate of the retro-[2+4] reaction is more nearly comparable to that of dehydrogenation in tetralin, resulting in competitive formation of 6 and 7 with 2 and 3. If the retro-[2+4] reaction in tetralin

is concerted, disruption of the aromatic nature of the ring system may give rise to a higher energy transition state for ethylene loss. If the concerted pathway is shunned due to this situation, a stepwise carbon-carbon bond cleavage with subsequent loss of ethylene may be occurring. In either case, one would expect a higher activation energy for the ethylene-loss channel, one more nearly comparable to that of dehydrogenation. The observation of o-allyltoluene, the disproportionation product from the intermediate in a stepwise process, indicates that the non-concerted reaction is energetically feasible. The occurrence of 1,2- instead of 1,4-dehydrogenation is perhaps not surprising since again the aromatic nature of the ring system must be destroyed for a concerted 1,4-hydrogen elimination to occur. Questions as to the energetics of these processes and their mechanisms are under active investigation.

Acknowledgements. We gratefully acknowledge the joint research support of the Division of Advanced Systems Materials Office of Advanced Isotope Separation, and the Divisions of Basic Energy (Chemical Sciences) and Fossil Energy (Advanced Research), U. S. Department of Energy, all under contract No. W-7405-Eng-48.

Michael R. Berman, Paul B. Comita,
C. Bradley Moore, Robert G. Bergman
Materials and Molecular Research Division,
Lawrence Berkeley Laboratory, and
Department of Chemistry, University of
California, Berkeley, California 94720.

References and Notes

(1) a) A. G. Loudon, A. Maccoll, and S. K. Wong, J. Chem. Soc. (B), 1733 (1970); b) R. J. Hooper, H. A. J. Battaerd and D. G. Evans, Fuel, 58, 132 (1979); c) P. Bredael and T. H. Vinh, Fuel, 58, 211 (1979); d) B. M. Benjamin, E. W. Hagaman, V. F. Raaen and C. J. Collins, Fuel, 58, 386 (1979); e) T. Gangwer, D. MacKenzie, and S. Casano, J. Phys. Chem., 83, 2013 (1979).

(2) For example, compare references 1a and 1e for the static pyrolysis results.

(3) The minor products have been tentatively identified as toluene, ethylbenzene, 1,4-dihydronaphthalene, and o-ethylstyrene. Traces of other unidentified aromatics were also observed. In nearly all experiments, none of the above products amounted to more than one percent of the total reaction mixture.

(4) See M. D'Amore, R. G. Bergman, M. Kent and E. Hedaya, Chem. Comm., 49 (1972), for a description of the flow reactor.

(5) A sample cell consisted of a 2 cm i.d. by 20 cm long pyrex cell with KCl windows mounted at the Brewster angle. The cell was pumped to $<10^{-5}$ Torr on a grease-free vaccuum line and was pressured to 0.325 Torr of **1** for all photolysis experiments. Pressures of all gases were measured with a capacitance manometer.

(6) The laser pulse consisted of a 100 ns pulse followed by a 1 μs tail with an approximately 50:50 energy distribution

between the pulse and tail. The energy per pulse was 1.3 Joules.

(7) A 15 cm focal length NaCl lens was used to focus the beam. During a photolysis, the focal point was located at approximately the midpoint of the cell. The laser beam was attenuated by placing a gas cell containing SF_6 in front of the photolysis cell. The intensity was varied by varying the pressure of SF_6. The energy density at the focal point was 46 Joules/cm^2 at 0.8 Joules/pulse and 23 Joules/cm^2 at 0.4 Joules/pulse.

(8) At low fluences **7** was not observed, presumably due to lack of secondary decomposition of **6**.

(9) Phenylacetylene was identified by GC-MS of the photolysis mixture. It was not a product in the flow pyrolysis or sensitized photolysis. In the direct irradiation experiments, this product could result from dehydrogenation of vibrationally excited styrene.

(10) K. J. Olzyna, E. Grunwald, P. M. Keehn, and S. P. Anderson, Tet. Lett., 1609 (1977).

(11) The photolysis cell for the sensitized photolysis was 4.5 cm i.d. by 4 cm long. The energy/pulse ranged from 0.11 to 0.27 Joules/pulse and the beam diameter was 0.7 cm. The energy absorbed ranged from 0.024 to 0.14 Joules/pulse. The variation in beam intensity was achieved as described in reference 7.

(12) The initial temperature after a pulse was calculated assuming all absorbed energy is statistically distributed

among all of the degrees of freedom of SiF_4 and **1**.

(13) Photolysis condition[10]: 300 shots, 0.27 Joules/pulse, 5 Torr SiF_4 and 0.325 Torr **2** or **6**.

(14) Minor products were 1,4-dihydronapthalene (7% of product), **1** (5%), **3** (3%), and six unidentified products (total 5.9%).

(15) Tetralin labelled with deuteria in the benzylic positions was obtained by treating **1** with D_5-dimsyl anion in D_6-dimethylsulfoxide.

(16) Analyses for isotope distribution in each of the pyrolysis products of **1-d$_4$** were obtained by GC-MS. The mass spectra were obtained at 15 eV.

(17) D. C. Tardy, R. Ireton, and A. S. Gordon, J. Am. Chem. Soc., 101, 1508 (1979).

(18) The surface to volume ratio was increased by a factor of four by using a cell 4.5 cm i.d. by 1 cm long.

Scheme I

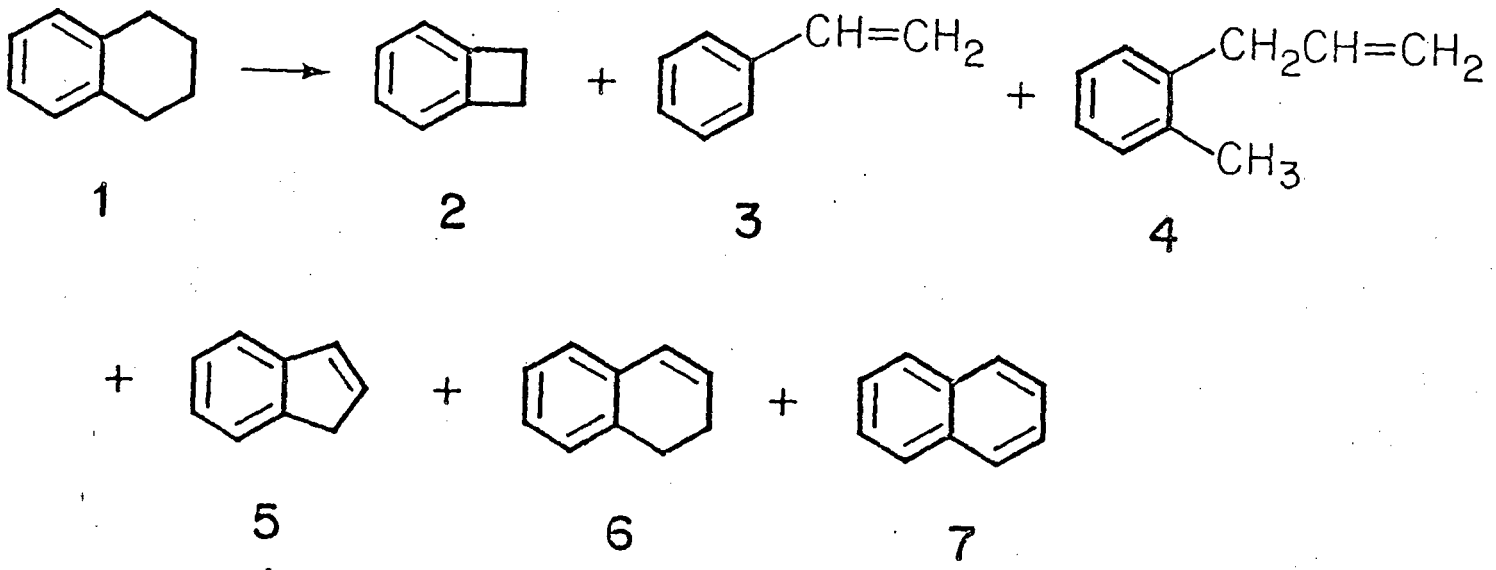

Table 1. Product distribution for thermal reaction of 1.

Conditions	Products (%) 2	3	4	5	6	7	other	% conversion
Flow pyrolysis, 1 atm. N_2, quartz reactor, 750°C.	2.4[a,b]	18.3	0.5	17.5	10.7	45.8	4.2	74.
Vacuum flash pyrolysis, 0.05 Torr, quartz reactor, 750°C.	34.7	9.9	7.9	4.1	31.8	8.2	3.4	3.
Multiphoton excitation, 0.325 Torr 1, energy/pulse 0.4 Joules, 13,020 pulses.	72.6	11.7[c]	3.4	4.2	6.2	0.0	2.0	0.
Multiphoton excitation,[d] 0.325 Torr 1, energy/pulse 0.8 Joules, 2790 pulses.	54.8	19.7[c]	2.6	5.5	9.0	trace	8.4	0.
SiF_4 sensitization,[11] T_{max} = 700°C, 5 Torr SiF_4, 0.325 Torr 1, 4960 pulses.	58.5	8.3	20.8	2.2	10.3	0.0	0.0	1.
SiF_4 sensitization,[11] T_{max} = 1540°C, 6 Torr SiF_4, 0.325 Torr 1, 180 pulses.	38.2	20.1	8.4	9.4	15.5	5.6	2.8	7.

[a]Numbers are percent of total product found. [b]All data have been corrected for FID response. [c]Includes phenylacetylene response. [d]Visible emission in the focal region was observed in this experiment.

Table 2. Deuterium labeling in products from photolysis of 1-d_4[a].

Product	% of total mixture	Isotopomer (%) d_4	d_3	d_2	d_1
2	57.8	100[b,c]	0	0	0
3	10.6	32	8	29	31
4	8.2	100	0	0	0
5	4.2	0	42	43	15
6	12.8	10	83	7	0
7	2.3	0	1	95	4

[a]Photolysis conditions: 1-d_4 (0.325 Torr) was irradiated with 300 pulses, 0.27 Joules per pulse, with 5 Torr SiF_4. T_{max} was 1240°C. [b]The numbers are the percent of product with the indicated number of deuterium atoms as determined by GC-MS analysis.[16] [c]The data are corrected for ^{13}C natural abundance and 98.7% deuterium incorporation in 1-d_4.

Characterization of the Degradation of Hydrodesulfurizing Catalysts

D. P. Whittle,* K. Stanley,* and A. V. Levy*

ABSTRACT

The loss of catalytic activity by hydrodesulfurizing hydrogenation catalysts during service has been studied by examining a number of catalyst pellets after different periods of exposure. A surface scale forms as an outer shell around the pellets. Metallic impurities, principally V or Fe and Ti, depending on the source of the oil being treated, tend to segregate within this scale. In addition, the scale also contains relatively high concentrations of S and Mo, presumably as MoS_2. The Mo concentration is usually higher than that measured in the original catalyst-pellet. The scale is not removed during regeneration; indeed, in some instances, it appears to increase in thickness.

Keywords: Catalysts, degradation, sulfidation

---

*Materials and Molecular Research Division, Lawrence Berkeley Laboratory, University of California, Berkeley, CA 94720.

INTRODUCTION

Hydrodesulfurization hydrogenation catalysts have become increasingly important as supplies of clean, low-sulfur fossil fuels, principally oil, become increasingly scarce. Low-sulfur fuels may be retrieved from the heavier feedstocks, such as those derived from coal by liquefaction, or potentially from oil shale. However, a catalytic desulfurizing treatment is a necessary part of the overall upgrading process, and there is a high level of current interest in identifying the most efficient catalyst, and in understanding its eventual loss of catalytic activity.

In tests of 150 catalysts, both commercial and industrial, CoMo and NiMo catalysts on an alumina or alumina-silica support have been shown to give the best overall performance with respect to a high level of catalytic activity over their lifetimes.[1] These catalysts are manufactured by impregnating ~~an alumina-silica~~ the support with a suitable metal salt, ammonium paramolybdate in the case of Mo, followed by extrusion into pellet form and calcination. During calcination, the catalytic metals form oxides. Ideally, these metal oxides should be evenly distributed throughout the pellet, but there is recent evidence that under certain conditions this may not be the case.[2] The catalysts are then sulfided with a suitable mixture of H_2S-H_2 gas (1:50) to give metal sulfides, the temperature in the sulfiding reactor being increased slowly up to a maximum of about 400°C, thus ensuring that the higher sulfides are formed. These sulfides slightly degrade the catalytic activity of the surface, but increase their overall useful lifetime.

Research by Gates et al.[3] to determine the mechanism and kinetics of hydrodesulfurization used dibenzothiophene as the sulfided hydrocarbon, which is considered to be better than thiophene as a model for the sulfur-containing species in a heavy feedstock. The Gates group used a conventional CoO-MoO/α-Al_2O_3 as catalyst and showed that the desulfurization was much faster (by 3 orders of magnitude) than the partial hydrogenation of the dibenzothiophene, indicating that desulfurization does not require hydrogenation of the aromatic ring prior to sulfur removal. What makes their results even more relevant is that the experiments were run at temperatures and pressures close to those of commercial operating plants: 300^{o}C and 100 atm. Other factors affecting the pseudo-first-order reaction rate are as follows:

(i) increasing the H_2S partial pressure increased the rate of hydrogenation;

(ii) the use of Ni catalysts (Mo-Ni or W-Ni) also increased the hydrogenation activity, and

(iii) methyl substitutes on the benzyl rings of dibenzothiophene alter the product distribution, but only if the methyl group is on the carbon which is β to the sulfur, suggesting a strong steric hindrance for the desulfurization step.

In industrial applications, it is important to minimize the rate of hydrogenation so as to conserve H_2 for the desulfurizing step, thus leading to higher yields per mole of H_2.

Equally important is the structure or pore volume distribution of the catalyst, or more specifically the ~~alumina-silica~~ support. To

give a high product-yield/wt catalyst, catalyst pellets must have very high surface areas, and it has been observed that a unimodal (single pore size) catalyst is not as efficient as a bimodal or multimodal catalyst. Because feedstocks can consist of molecules with a wide size variation, a small, unimodal catalyst can become clogged by the formation of coke through hydrogenation and polymerization of large aromatic molecules such as asphaltenes (50Å) and porphyrins (250Å-500Å). However, a catalyst with a large, unimodal structure would have a lower catalytic surface area, hence decreasing the yield. The development of the bimodal catalysts allows transport of large molecules onto active sites while maintaining a relatively large surface area. Suggestions[4] for an optimal distribution of a multimodal catalyst structure include a distribution where 60 percent of the pores have a diameter between 100Å and 200Å, at least 5 percent of the pores are <40Å, and at least 5 percent are >500Å.

It is clear then, that while the important characteristics of desulfurization catalysts are becoming understood, rather less is known about the degradation of the catalytic activity during operation and subsequent regeneration. This report describes preliminary research aimed at identifying the changes which take place during service on the catalyst surface and the formation of contaminant layers. A number of catalysts at various stages of use have been examined in detail, and the experimental procedures, methods of analysis, and results are presented. The final section contains recommendations for future research.

SAMPLE HISTORY

Samples of two types of catalyst were studied:

(i) Harshaw 618X - an experimental unimodal Ni-Mo catalyst which had been used to hydrodesulfurize a solvent-refined coal feedstock;

(ii) American Cyanamid HDS1441B - a unimodal Co-Mo catalyst which had been used to hydrodesulfurize crude oil feed.

Both types of samples were obtained from ~~the~~ Mobil Research and Development Corporation.

The Harshaw catalyst (hereafter referred to as HAR) was received in fresh and spent (used) conditions in late 1978. A portion of the spent HAR was air-regenerated at Lawrence Berkeley Laboratory (LBL).

Two sets of samples of the American Cyanamid catalyst (subsequently referred to as HDS(1) and HDS(2), respectively) were received, the first set in late 1978, the second in May 1979. The first set was received in fresh, spent, and air-regenerated conditions. The air-regenerated HDS 1441 (identified as HDS(1)-regen.-Mobil) operated in Lagomedio Atmospheric Resid (a heavy oil) for 13 days before regeneration. After regeneration it still contained 0.5 percent coke residue. The HDS(1)-spent was used in Arab Light Vacuum Resid for 20 days. A portion of HDS(1)-spent was air-regenerated at LBL, and is identified as HDS(1)-regen.-LBL. Note, therefore, that the samples in set (1) are not necessarily from the same supply of catalyst pellet, nor have the used and used/regenerated catalysts seen the same service conditions.

Samples in set (2) form a more consistent set: they were received from Mobil in fresh, sulfided-fresh (before use they are given a pre-sulfiding treatment as indicated earlier), spent, and regenerated forms. Table I lists the various samples examined and summarizes service exposure times, regeneration conditions, etc.

EXPERIMENTAL PROCEDURE

Sample Preparation

Samples were handled with tweezers, but no other special precautions were taken. The following method for cross-sectional examination of the pellets was developed. Four phenolic discs measuring 3/4" diameter by 1/8" thick were cemented together with epoxy to form a support 1/2" high and 3/4" diameter. For the HDS pellets a No. 67 drill bit was used to drill 5-10 holes across the face of the mount, each hole being drilled to a depth of approximately 3/32". The pellets were loosely fit into two holes, an effort being made to find pellets of approximately the same length. A similar procedure was adopted with the HAR pellets, but using a 1/16" drill.

Various methods were used to mount the pellets for scanning electron microscopy (SEM) and electron probe microanalysis (EPMA). Only Bakelite, Lucite, and epoxy resins are suitable as mounting media for EPMA. Bakelite was tried, but unsuccessfully since a soft mounting medium is desirable to prevent the pellet "digging out" from the mount. Vacuum-impregnated epoxy was tried with mixed results. Although the material is soft enough to minimize digging out of the catalyst samples, the epoxy appeared to interact chemically with the pellet. Careful measuring and mixing of the hardener and resin might help eliminate this problem and is worth pursuing: this mounting procedure has the advantage of being cold setting and does not require pressure.

Transoptic (Lucite) mounting material was used for the majority of samples. A phenolic mount, usually containing 5 pellets, was placed in the Pneumet I mounting press; then 1-1/2-2 measures of Lucite powder were added, the Pneumet closed, and heat applied for 10 minutes to melt the Lucite powder. After this, a low pressure, not greater than 100 psi, was applied with heat for a further 15 minutes. The mount was then cooled to room temperature, and the edges beveled to prepare for grinding and polishing.

During grinding and polishing only water was used as lubricant: organic lubricants appeared to lead to cracking of the pellets, although the exact cause has not yet been fully determined. Development of pressure during mounting or curing, or the grinding and polishing operations could all be contributing factors. Alternatively the pellets could already have been internally cracked before service, perhaps by the extrusion process. However, recent studies[4] suggest a new mounting procedure which seems to eliminate cracking. This procedure will be discussed later.

Mounted samples were ground through 180, 240, 320, 400, and 600 grade grinding papers and polished with 1μm alumina in water, with a final polish on finishing-grade alumina. The polished samples were then ultrasonically cleaned for 4-6 minutes. Samples to be examined in the SEM were sputtered with Au for 1 min at a current of 10μA with the sputtering chamber backfilled with A to a pressure of 180 Torr.

Methods of Analysis

In addition to conventional metallographic examination under the optical microscope, four other techniques were used: X-ray diffraction, SEM, EPMA (including energy dispersive analysis, or EDAX) and surface area determination by BET analysis.

X-ray diffraction analysis provided virtually no information: the average grain size of the alumina catalyst was too small. Possibilities exist for examining the surface scales by this method, and these will be discussed later.

SEM was used extensively: the edges and interior of pellets were examined at 500x magnification, or higher if necessary. X-ray maps of the cross sections examined were recorded for S/Mo (EDAX is unable to distinguish between these two elements), Ti, V, Fe, Al, Si and any other elements which appeared to be present in significant concentrations. Point analyses were also taken using the EDAX system at various locations through the section, and these were used to qualitatively assess the elemental distributions.

In conjunction with the SEM analyses, EPMA was also used primarily to separate the S and Mo X-ray spectra. Line analyses were carried out for three elements simultaneously, usually along directions normal to the pellet surface. At present the intensity data produced are only semi-quantitative.

BET surface area analyses were carried out to measure the change in surface area in fresh, spent, and regenerated pellets, and to determine whether the outer scale constituted a barrier against

gaseous diffusion which might lower the catalytic activity. In each determination the sample, approximately 40 mg, was outgassed with N_2 at about 170^{o}C for at least 1 h. This outgassing procedure serves to replace any gaseous species on the sample surface with N_2. At least three (BET) points were taken to get a surface area value. Each sample was tested until a statistically sound value was achieved with an error of around 2 percent. The surface area values listed in Table I represent typical values: surface areas of individual pellets may differ from these statistical values by as much as 5 percent.

RESULTS AND DISCUSSION

(a) Harshaw 618X

This catalyst had been used in a coal liquefaction process/product. Optical examination under low power of HAR-fresh showed that the pellets (average diameter 1/16") varied in surface color from a very faint blue to a cream-yellow. A similar variation in color was also noted in individual pellets. The majority of the pellets had smooth surfaces, but some were rather rough.

The HAR-spent pellets were evenly covered with a black layer of coke. This coke layer was seen to penetrate into the pellet to a uniform depth around the section. After regeneration at LBL, the black coke layer had apparently been removed and a light brown coating was present on the sample pellets. This was very thin in some places, allowing the whitish color of the freshly regenerated catalyst to show through. The interior of the pellets resembled the fresh pellets.

Figure 1a shows a typical section through a HAR-fresh pellet; the points where EDAX analyses (Figs. 1b and c) have been carried out are marked. EDAX analysis shows that Mo tends to concentrate slightly at the edge of the pellet, gradually decreasing to a steady-state concentration away from the interface. On the other hand, as far as can be detected using EDAX, the Ni concentration remains more or less constant. Al and Si were the only other elements detected by EDAX, these being present in the catalyst-supporting Al_2O_3. It is worth noting that these catalyst pellets had not been given the preliminary sulfiding treatment and both Mo and Ni would be present as oxides;

after the pre-sulfidation treatment Mo is present as MoS_2 which gives a black coloration to the surface.

Examination in section of a spent catalyst pellet (HAR-spent) reveals the presence of a compact scale around the surface (Fig. 2a). EDAX analysis of this scale (point 1 in Fig. 2a) indicates significant concentration of S/Mo, Ti, Fe, Ca and Ni (Fig. 2b). The Fe, Ni and Co are isolated on the very edge (1 μm) of the scale. Figure 2c shows the EDAX analysis from point 2 in Fig. 2a which is about 10 μm from the edge, and essentially only Al, S/Mo and Ni are present. EPMA traces for S, Mo, and Ni are shown in Fig. 3. In Fig. 3a there is a significant concentration of S in the outer 10μm of the pellet with a less significant build-up of Mo and Ni. All three elements are relatively uniformly distributed throughout the remainder of the pellet. In contrast, along the profile shown in Fig. 3b there is a substantial build-up of both S and Mo in the outer 20 μm of the pellet. In fresh pellets, Mo, S, and Ni are uniformly distributed through the pellet (Fig. 3c). The increase in S and Mo in the surface region of the spent pellet compared to the fresh pellet is of major importance and requires further study.

Figure 4 shows a section through a pellet that was regenerated at LBL (HAR-regen.-LBL). The scale on the surface is thicker in comparison with that before regeneration (Fig. 2) and also appears to be more particulate in nature. Figures 4b, c and d are X-ray maps showing the distributions of Fe, S/Mo and Ti respectively. Fe is isolated in the surface layer, which contains only small amounts of

S/Mo and Ti. Ti is concentrated just below the scale layer, as is the S/Mo. EDAX analyses of the points indicated on Fig. 4a are presented in Fig. 4e to 4j. Within the surface scale there are relatively high concentrations of Fe, S/Mo and Ti; Fe is mainly concentrated within this scale region; however, Ti concentrations can be detected well away from the surface scale as verified in the X-ray map of Fig. 4d. The S/Mo appears to be more evenly distributed than in the spent pellets. There are also traces of Ca in the surface scale. Figure 5 shows EPMA concentration profiles through the scale, and it is clear that the Ti is concentrated near the surface, while Mo and S are distributed throughout the catalyst pellet. The change in the surface concentration of S and Mo from the high levels in the spent catalyst pellets to the low levels in the regenerated ones--similar to the difference between the spent and fresh pellets--is significant and requires further study.

(b) HDS 1441

In discussing the results of this catalyst it must be remembered that the catalyst samples were used in a crude-oil refining process and were from different sources as indicated in Table I. Its behavior will be somewhat different from the Harshaw 618X catalyst, used in a coal liquefaction process. The fact that the pellets received for analysis were exposed to different crude oils will also cause some difference in the behavior of the pellets. Visual examination of HDS(1)-fresh showed an uneven, deep blue color, with some pellets being also black around the edges. The blue coloration lightens

toward the center of the pellet section, making it appear as if there were a shell of active material possibly caused by calcination of the catalyst after impregnation.[2] The second set of samples of this catalyst, HDS(2)-fresh, were identical in appearance to HDS(1)-fresh.

Figures 6a and b show sections through the fresh catalyst, HDS(1)-fresh, and Figs. 6c and d show a spent and regenerated catalyst, HDS(1)-regen.-Mobil. The presence of a surface scale around the catalyst pellet in the regenerated condition is clearly evident. No such scale is present on the fresh catalyst. The interior of the catalyst pellet is similar in both samples.

Figure 7 shows that there is some interaction between the surface of the catalyst and epoxy resins when these are used as mounting material. However, this is only the case when the surface of the pellet is not covered with a surface scale (Fig. 7a). The upper surface in the micrograph is where the pellet has been fractured and so there is no surface scale. In other samples cracks appear in the pellets. In Fig. 7b it appears that the crack developed in the pellet during service since a scale has formed down the sides of the crack, and this scale has prevented interaction with the epoxy resin mounting medium penetrating down the crack. In the pellet shown in Fig. 7c, cracking presumably occurred during the mounting operation since there is no scale on the crack surface and where the epoxy has penetrated, it has reacted with the catalyst. The behavior of the mounting compound with the catalyst pellet only in areas that do not have a surface scale may be indicative of the de-activating nature of the scale.

Figure 8 shows a section through HDS(1)-fresh, and the structure appears reasonably uniform throughout the section. There are areas which are rich in Si (Fig. 8b), but this is present as 3.7 percent SiO_2 in the Al_2O_3 support. Figure 9 shows another section of HDS(1)-fresh, and the point EDAX analysis shows that there is a slight concentration of S/Mo near the surface, but that this reaches a steady value about 10 μm below the surface; Co shows similar behavior, although of course its concentration is much lower.

The HDS(1)-spent sample, which had been used in an Arab Vacuum Light Resid for 20 days, had a scale on the surface of the pellet some 25 μm in thickness in places. Figure 10 shows a typical cross-section together with a number of point analyses through the scale and pellet. Vanadium was present in significant concentrations in the outer 30 μm from the edge of the sample, but was negligible at distances greater than 75 μm from the surface. EPMA concentration profiles are shown from a different pellet in Fig. 11. In this case there are appreciably high concentrations of V near the surface, but also occasionally at depths of 70 μm below the surface. In this particular trace the sulfur concentration showed a rather irregular pattern. This was also true with other pellets of the same sample where sometimes the sulfur showed a maximum concentration of 8-10 μm from the surface, and in other instances at 35 μm from the edge.

The Mo concentration was always highest anywhere from 50-75 μm from the edge and always corresponded to a large, if not the maximum, S concentration.

Figure 12 shows concentration profiles through the scale in the second set of spent catalysts of this type, HDS(2)-spent. These had also been used in an Arab Light Vacuum Resid, but for 65 days. In spite of this longer exposure the concentration of V was somewhat lower in the scaled surface, although V did appear to penetrate deeper into the pellet. Mo and S concentrations were approximately uniform through the pellet.

Air regeneration of the HDS catalyst used in the Arab Light Vacuum Resid was carried out at LBL as indicated in Table I. EPMA across the sample, HDS(1)-regen.-LBL, is shown in Fig. 13. V is not removed by the regeneration process and is present up to 75 μm below the surface at concentrations similar to those observed in the unregenerated catalyst pellet. The high concentration of sulfur, however, appears to have been removed, while the distribution of Mo appears to be unaltered.

Some samples of the HDS-1441 catalyst which had operated in a Lagomedio Atmospheric Resid were also examined. Unfortunately no spent but unregenerated samples were available, but Fig. 14 shows a section through a sample which was regenerated after use by Mobil: HDS(1)-regen.-Mobil. The scale, although cracked in places, shows a high degree of compactness. V is again shown to be heavily concentrated in the scale and decreases with distance into the pellet; the S/Mo peak decreases similarly. Profiles obtained by EPMA are shown in Fig. 15 and there is a significant concentration of V down to about 80 μm below the surface, but S still seems to be concentrated near the surface in spite of the sample being regenerated.

CONCLUSIONS

Scales do form as an outer shell around the catalyst pellets during hydrodesulfurization service. Metallic impurities, principally V or Fe and Ti, depending on the source of the oil being treated, tend to segregate within this scale. In addition the scale also contains a relatively high concentration of sulfur and Mo, presumably as MoS_2. The Mo concentration is usually higher than that measured in the original catalyst pellet.

Whether the presence of this scale causes a decrease in the catalytic activity has not been demonstrated. Certainly, the scale is not removed during regeneration; indeed in some instances it appears to increase in thickness, although exact comparison between used and regenerated catalysts is difficult since it is not known whether the sample pellets come from the same batch.

There is considerable variation in observed behavior from one sample to another, and from area to area on the same sample surface. For example, in some cases, sulfur appears to be oxidized from the surface during regeneration, in some cases not. However, these preliminary results have shown the potential of a metallographic analysis that follows the build-up of metallic impurities and sulfur on the surfaces of catalyst pellets during hydrodesulfurization of the surface.

Further work must use catalyst pellets whose service history is well characterized, and it is proposed to expose catalyst samples in a laboratory-scale reactor in which the metal- and sulfur-contamination

levels in the oil feedstock and the exposure conditions can be controlled. In this way the parameters which affect scale formation can be identified. In addition, of course, it will be necessary to relate scale build-up on the pellet surface with loss of catalytic activity, and to identify the degradation mechanisms that are taking place.

ACKNOWLEDGMENTS

This work has been supported by the Division of Materials Science, Office Of Basic Energy Sciences, U. S. Department of Energy, under contract no. W-7405-Eng-48.

REFERENCES

1. K. K. Robinson, R. J. Bertolucini, L. G. Gutberlet, and D. K. Kim, Amoco Oil Company Annual Report AF-574, prepared for Electric Power Research Institute (RP 408-1), March 1978.

2. R. Srinivasan, H. C. Liu, and S. M. Weller, J. Catalysis 57, 87 (1979).

3. J. J. Stanulonis, B. C. Gates, and J. H. Olson, AICHE Journal 22, 576 (1976).

4. M. G. Thomas and D. G. Sample, Sandia Laboratories, SAND-79-0085, May 1979.

Table I
Catalyst Samples

American Cyanamid HDS 1441 - 1/32" Diameter pellets, Co-Mo on Al_2O_3

Properties: 2.7%CoO/15.3%MoO_3/3.7%SiO_2/ balance Al_2O_3
Surface area: 290 m^2/g
Pore volume: 0.596 ml/g.

Sample Designation	History
HDS(1)-fresh HDS(1)-spent	Used in Arab Light Vacuum Resid for 20 days.
HDS(1)-regen.-Mobil	Used in Lagomedio Atmospheric Resid for 13 days and regenerated in 0.7% O_2-99.3% N_2 at 0 psig for 2 h each at 316, 343, 371, 399, 427°C and 6 h at 454°C.
HDS(1)-regen.-LBL	Used in Arab Light Vacuum Resid for 20 days and regenerated in 2% O_2 - 98% N_2 at 1 atm. for 24 h at 400°C.
HDS(2)-fresh HDS(2)-S-fresh	Fresh catalyst sulfided in 2% H_2S - 98% A, 1.0 ft^3/h at 500 psig for 1 h each at 232, 288, 344°C and 2 h at 399°C.
HDS(2)-spent	Used in Arab Light Vacuum Resid for 65 days.
HDS(2)-regen.	As HDS(2)-spent but regenerated in 0.7 O_2-99.3 N_2 at 0 psig for 2 h each at 316, 343, 371, 399, 427°C and 6 h at 454°C.

Harshaw H618X

Properties: 2.7% NiO/14.8% MoO_3/balance Al_2O_3
Surface area: 140 m^2/g
Pore Volume: 0.6 ml/g
Average pore size: 172Å.

Sample Designation	History
HAR-fresh HAR-spent	Used in 50% W. Kentucky SCT-SRC.
HAR-regen.-LBL	As HAR-spent but regenerated in 2% O_2 - 98% N_2 at 1 atm. for 24 h at 400°C.

FIGURE CAPTIONS

Fig. 1. Section through fresh Harshaw H618X catalyst and EDAX analyses of the respective points indicated: HAR-fresh.

Fig. 2. Section through a spent Harshaw H618X catalyst and EDAX analyses of the respective points indicated: HAR-spent.

Fig. 3. EPMA traces through the surface layers on Harshaw H618X catalysts: (a) and (b) spent catalyst pellets, HAR-spent; (c) fresh catalyst: HAR-fresh.

Fig. 4. Section through Harshaw H618X pellet after regeneration: (a) SEM cross section: HAR-regen.-LBL; (b) Fe Kα X-ray map of section (a); (c) S/Mo Kα X-ray map of section (a); (d) Ti Kα X-ray map of section (a); (e) EDAX analyses of the respective points 1-6 indicated in section (a).

Fig. 5. EPMA traces through the surface layers on Harshaw H618X pellet after regeneration: HAR-regen.-LBL.

Fig. 6. Sections through American Cyanamid HDS 1441 catalyst pellets: (a) and (b) HDS(1)-fresh; (c) and (d) HDS(1)-regen.-Mobil.

Fig. 7. Sections through American Cyanamid HDS 1441 catalyst pellets, HDS(1)-regen.-Mobil.

Fig. 8. Section through American Cyanamid HDS 1441 catalyst in fresh condition: HDS(1)-fresh. (a) SEM micrograph; (b) Si Kα X-ray image of area shown in (a).

Fig. 9. Section through American Cyanamid HDS 1441 catalyst in fresh condition and EDAX analyses of the respective points indicated: HDS(1)-fresh.

Fig. 10. Section through a used American Cyanamid HDS 1441 catalyst and EDAX analyses of the respective points indicated: HDS(1)-spent.

Fig. 11. EPMA traces through the surface layers on American Cyanamid HDS 1441 catalyst in spent condition: HDS(1)-spent.

Fig. 12. EPMA traces through the surface layers on American Cyanamid HDS 1441 catalyst in spent condition: HDS(2)-spent.

Fig. 13. EPMA traces across the surface layers on American Cyanamid HDS 1441 catalyst after regeneration: HDS(1)-regen.-LBL.

Fig. 14. Section through surface layers on American Cyanamid HDS 1441 catalyst after regeneration and EDAX analyses of the respective points indicated: HDS(1)-regen.-Mobil.

Fig. 15. EPMA traces across the surface layers on American Cyanamid HDS 1441 catalyst after regeneration: HDS(1)-regen.-Mobil.

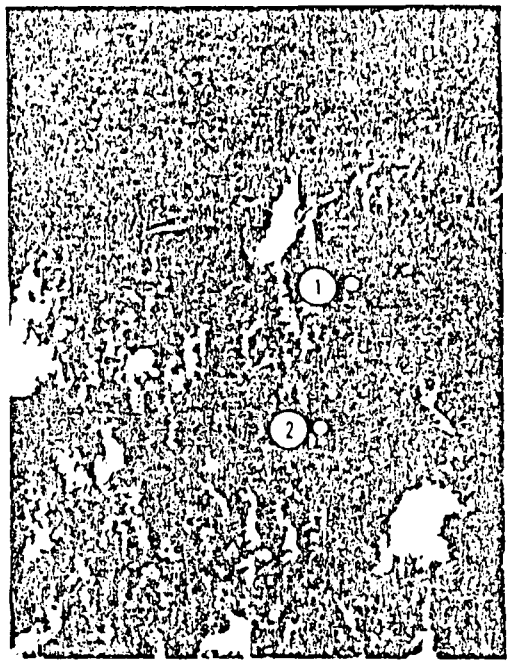

10 μm

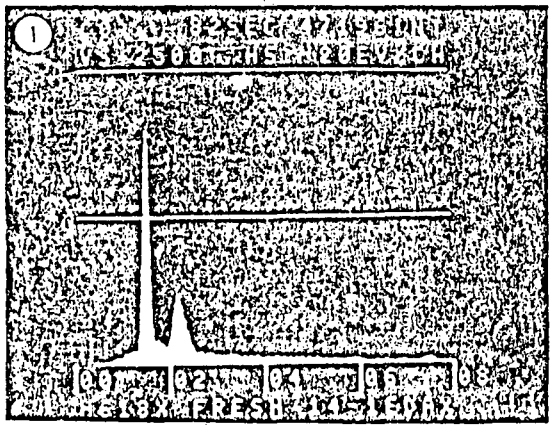

Al S/Mo Ni
Si

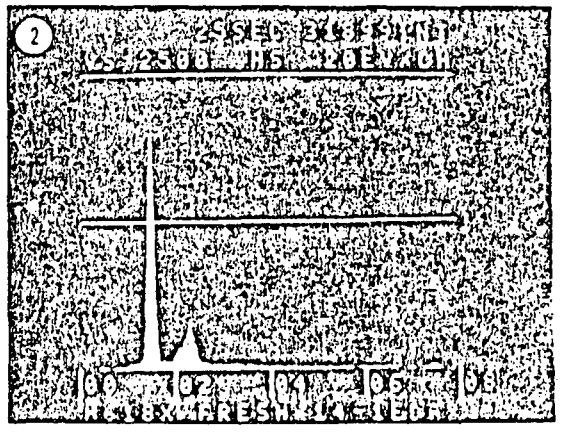

Al S/Mo Ni

Fig. 1

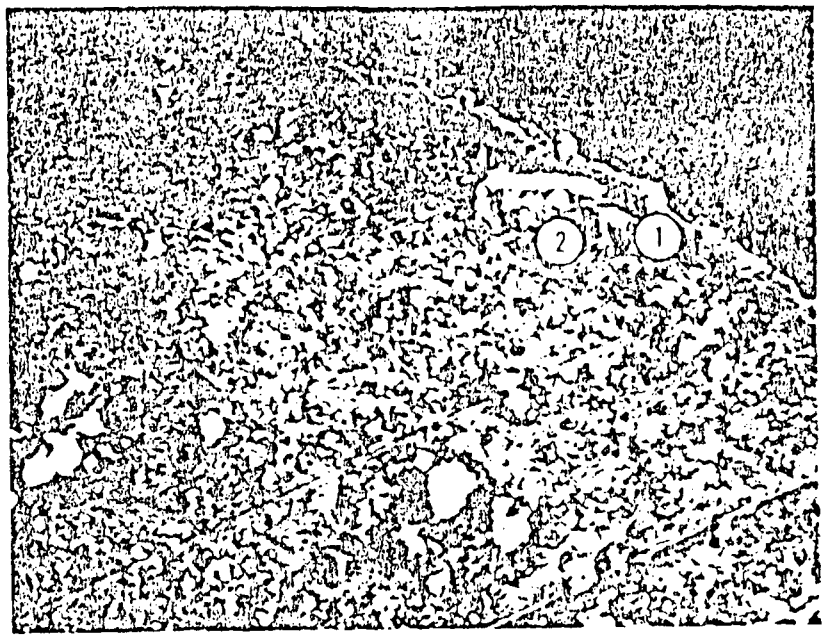

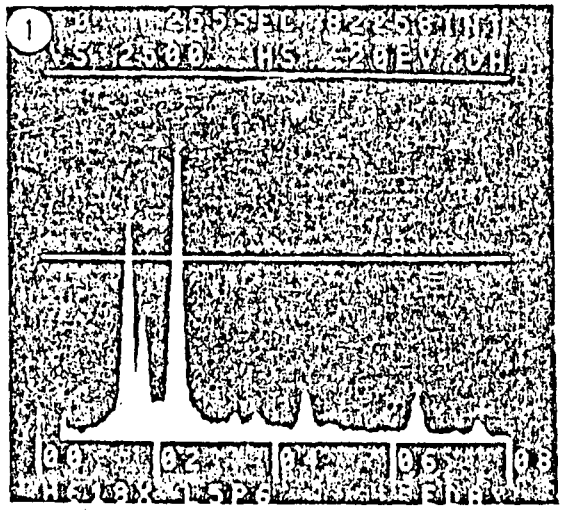

Al S/Mo Ti Fe Ni
Si Ca

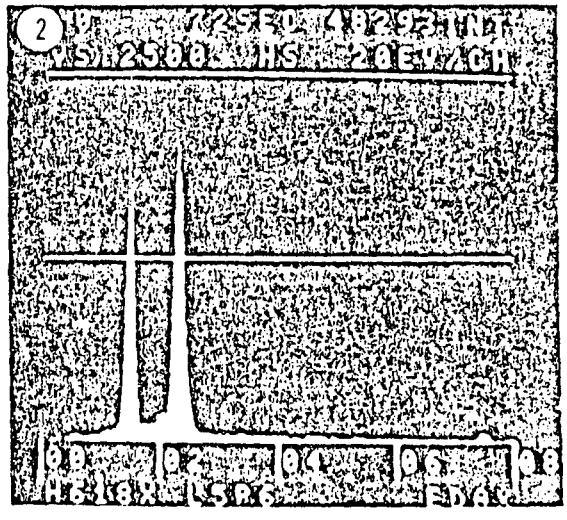

Al S/Mo Ni

Fig. 2

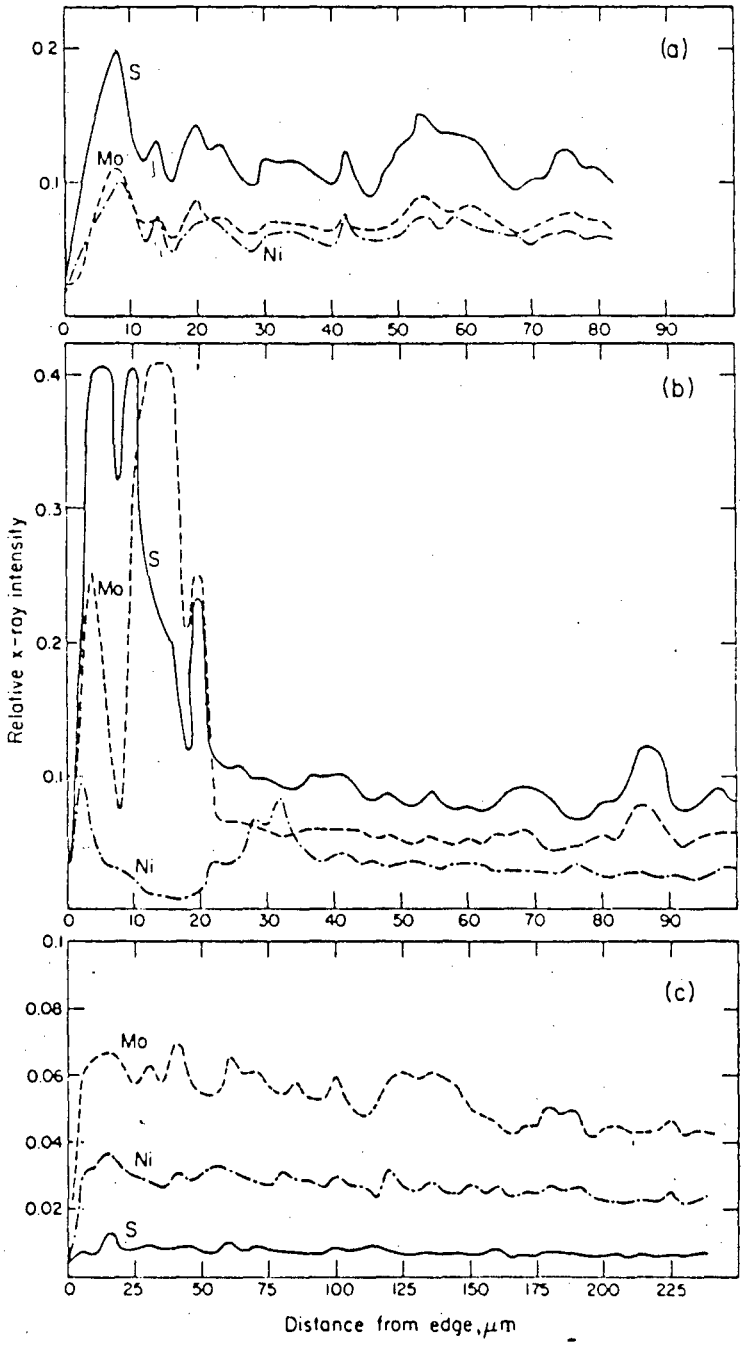
(a)
S
Mo
Ni
(b)
S
Mo
Ni
(c)
Mo
Ni
S
Relative x-ray intensity
Distance from edge, μm
XBL 802-185

Fig. 3

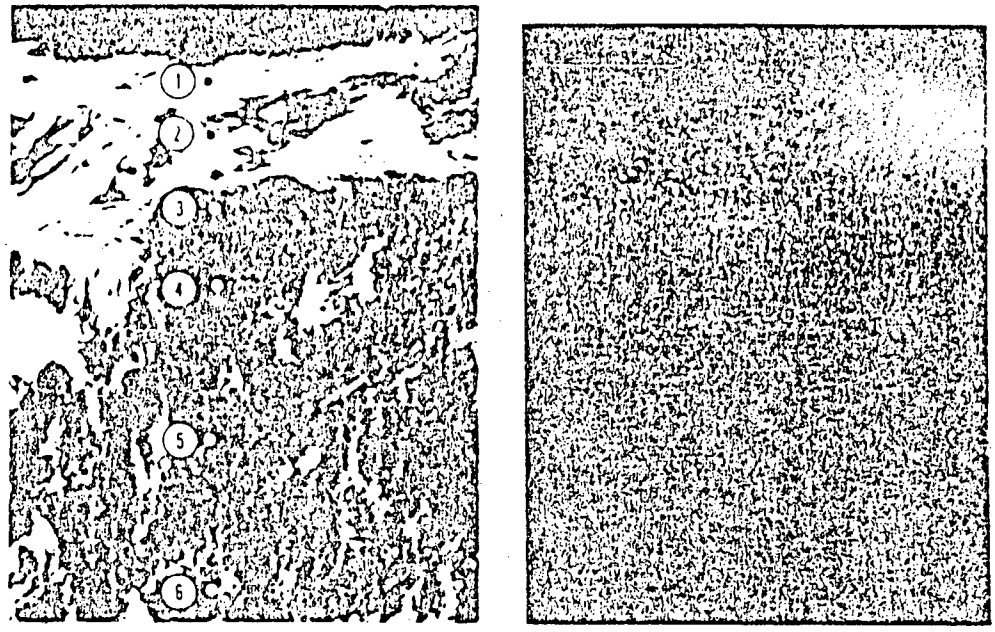

Fig. 4

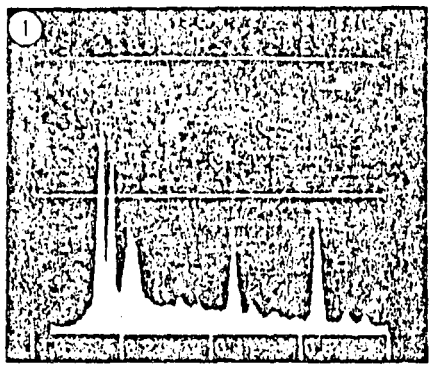

Al S/Mo Ti Fe Ni
Si Ca

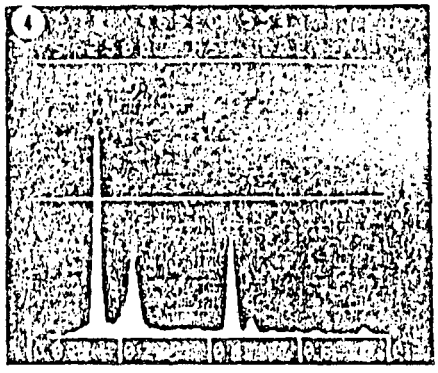

Al S/Mo Ti Fe Ni

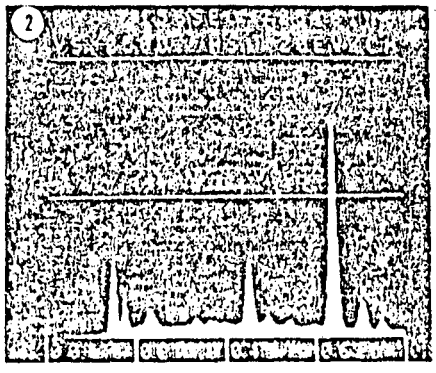

Al S/Mo Ti Fe Ni
Si

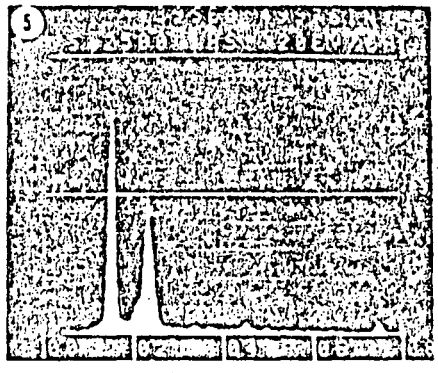

Al S/Mo Ti Ni

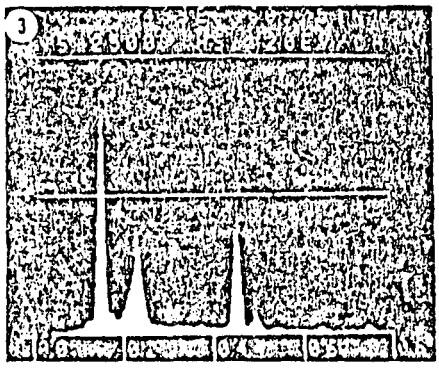

Al S/Mo Ti Fe Ni

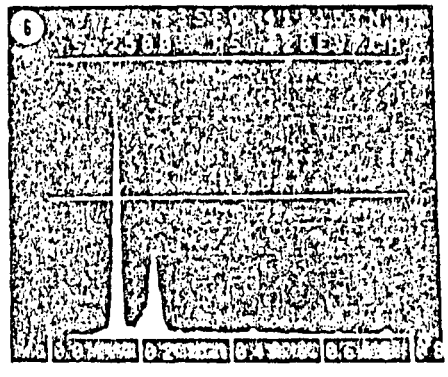

Al S/Mo Ti Fe Ni

(e)

Fig. 4 cont.

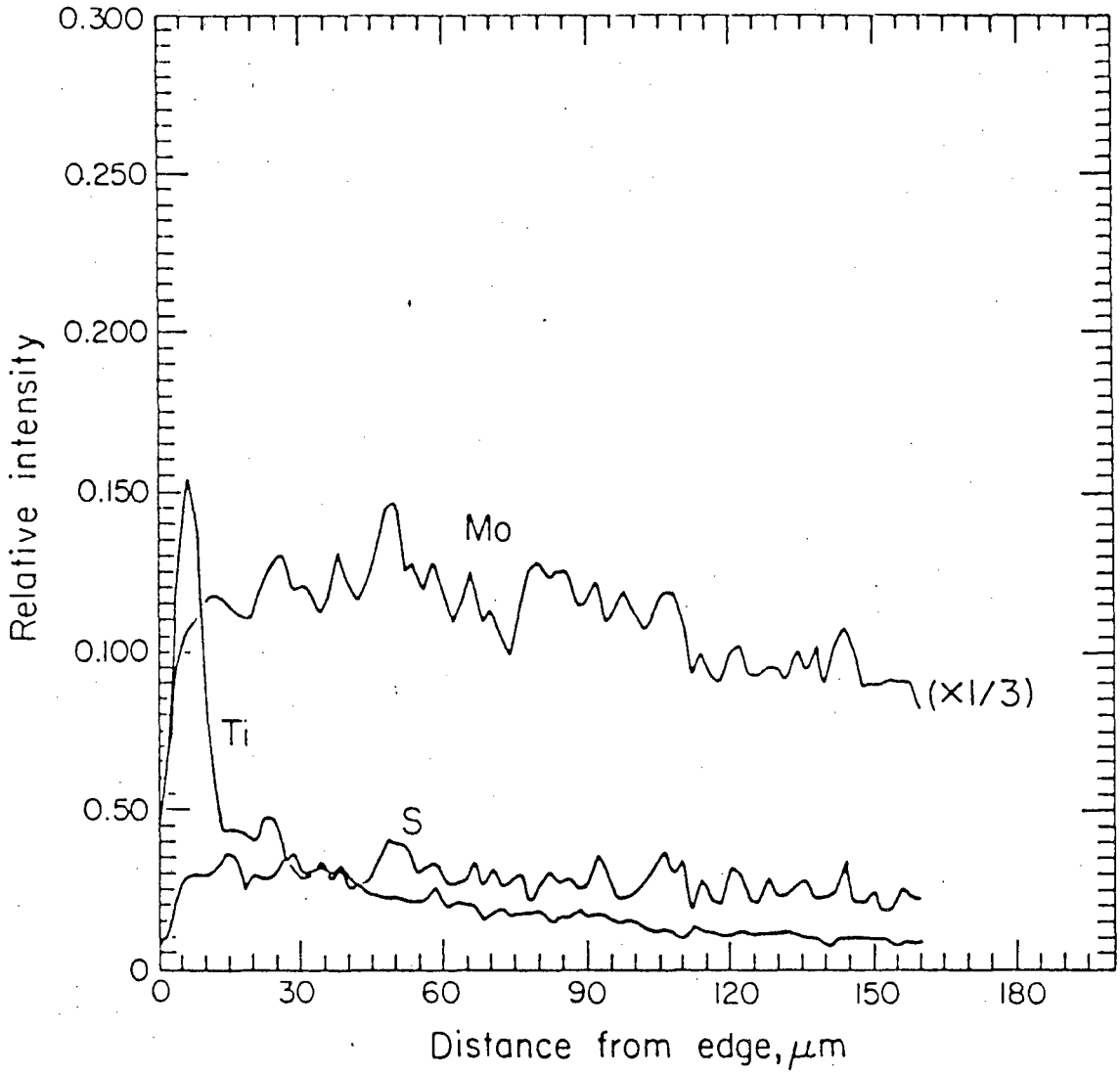

XBL 802-186

Fig. 5

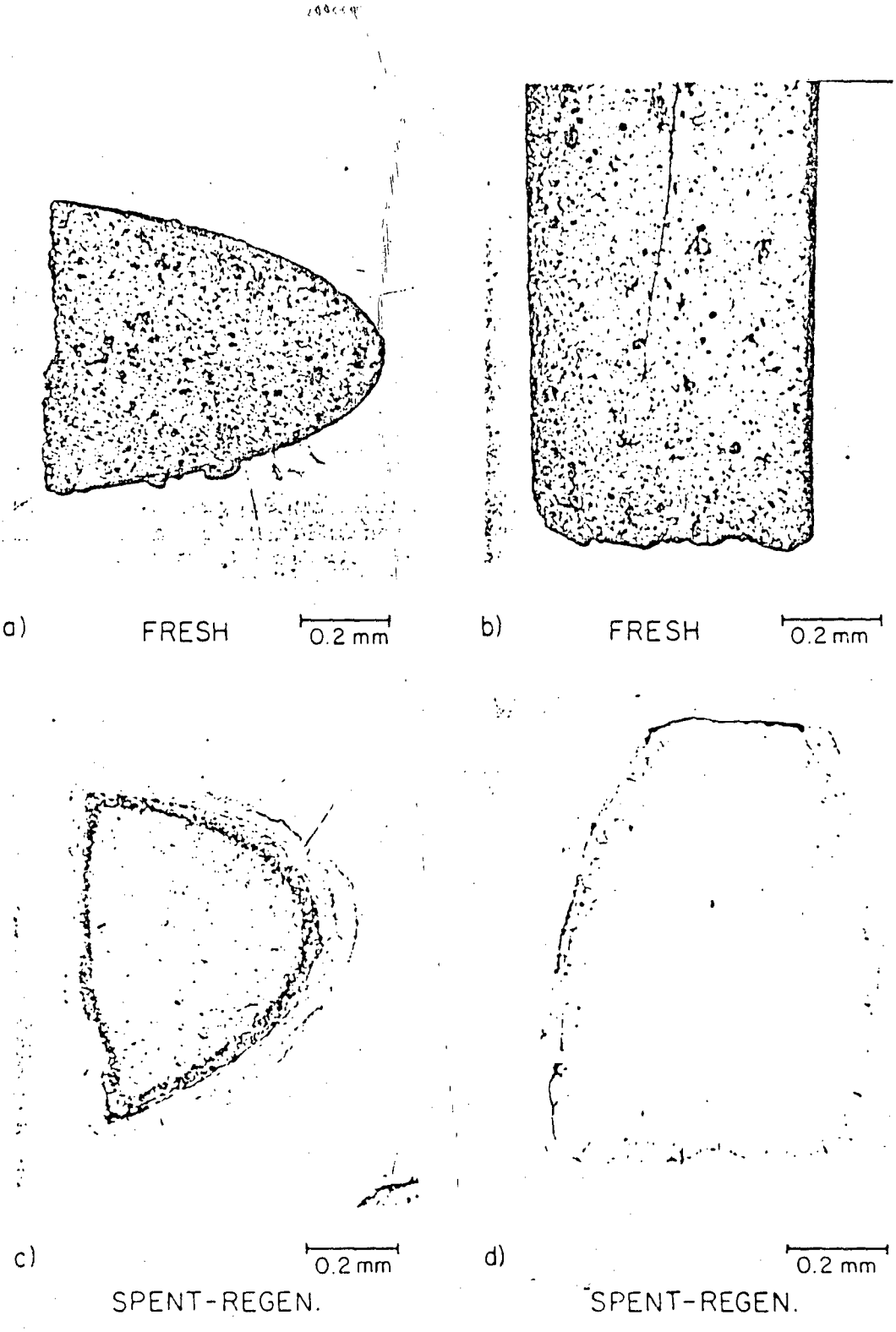
a)
FRESH
0.2 mm
b)
FRESH
0.2 mm
c)
0.2 mm
SPENT-REGEN.
d)
0.2 mm
SPENT-REGEN.

Fig. 6

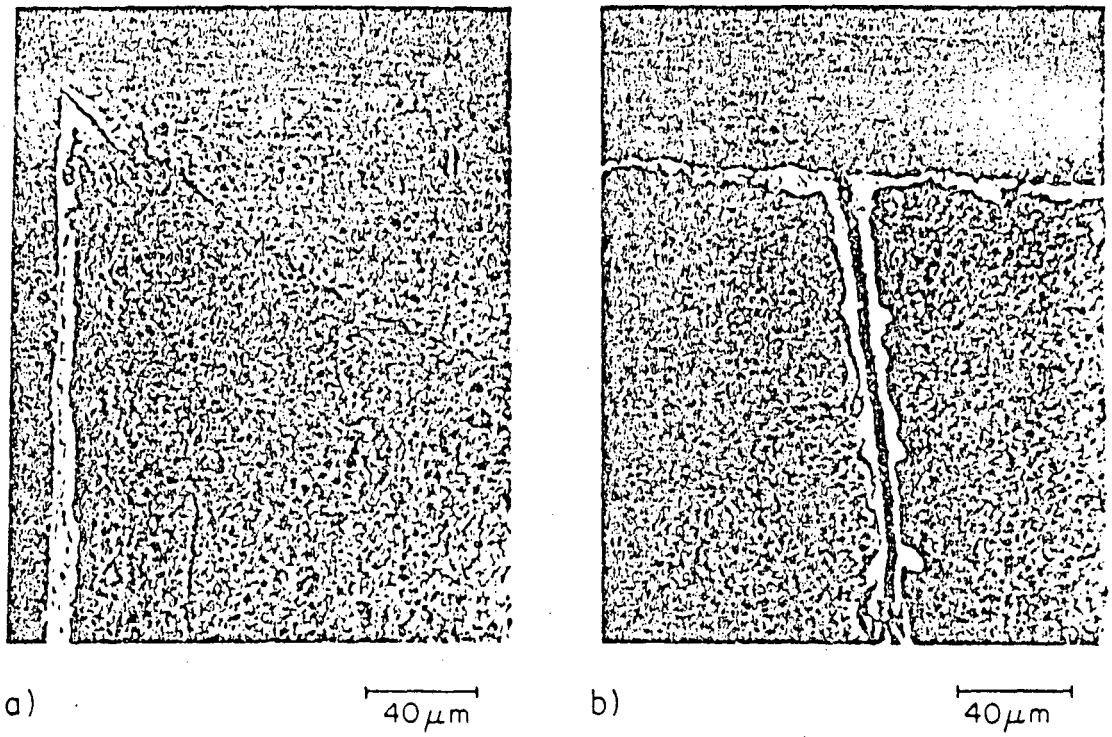

Fig. 7

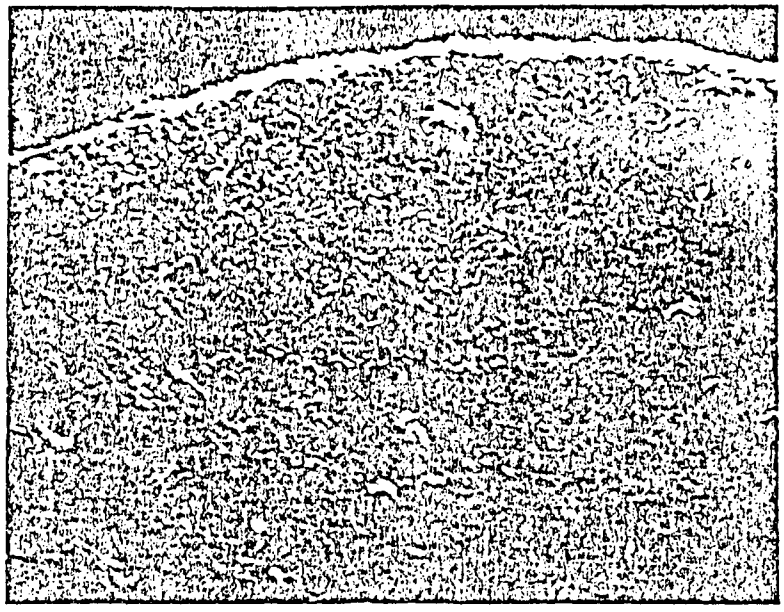

a)

40 μm

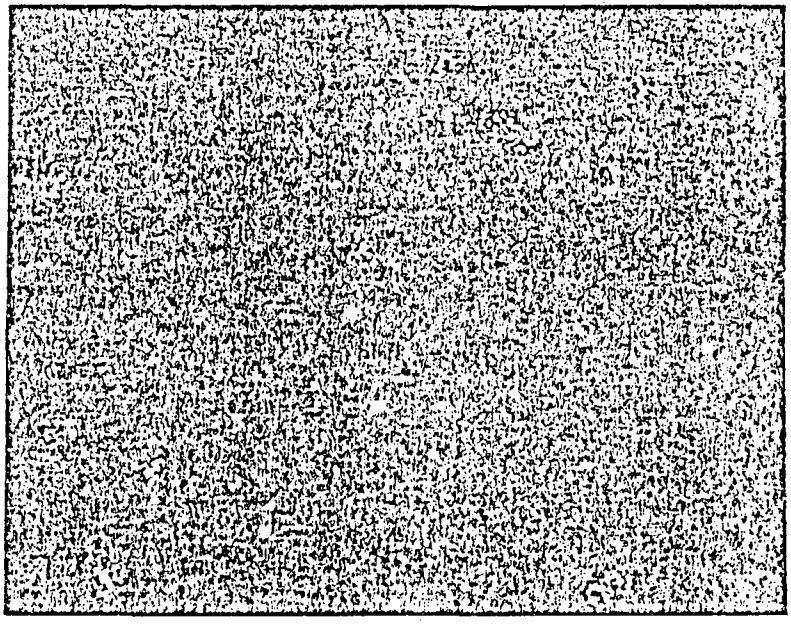

b)

Si

Fig. 8

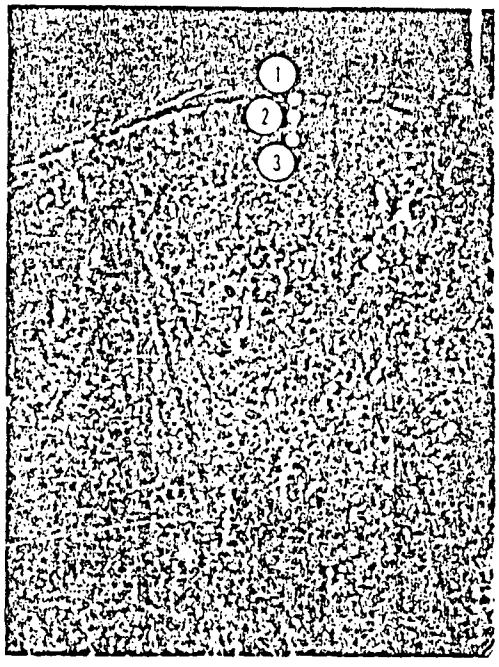

40 μm

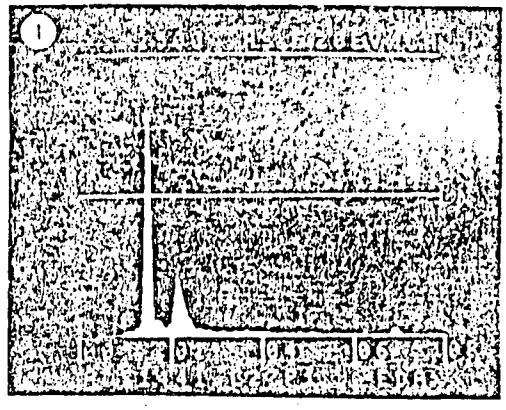

Al S/Mo Co

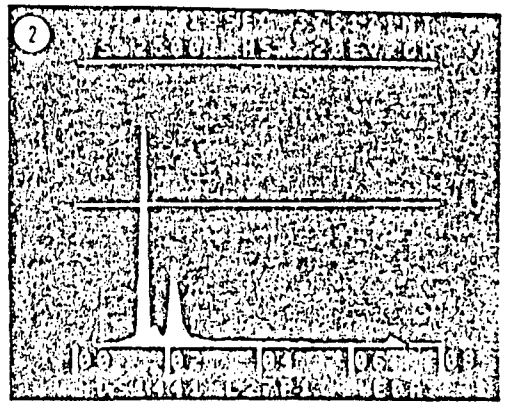

Al S/Mo Co

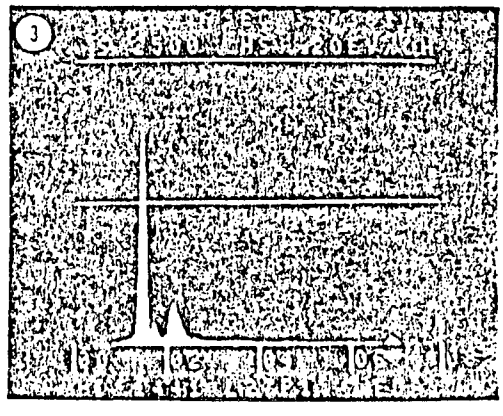

-Al S/Mo Co

Fig. 9

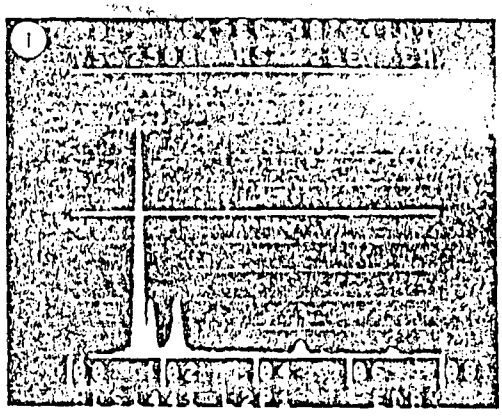

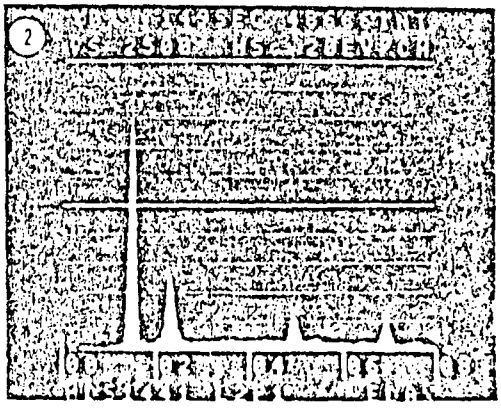

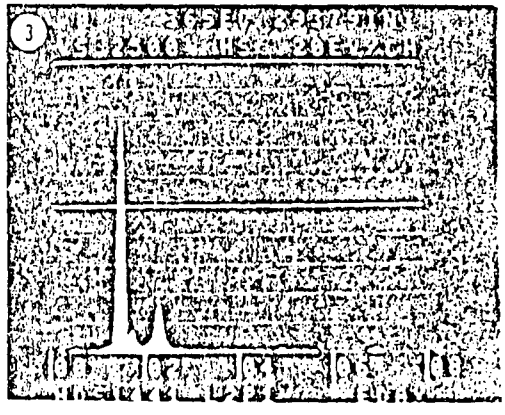

Fig. 10

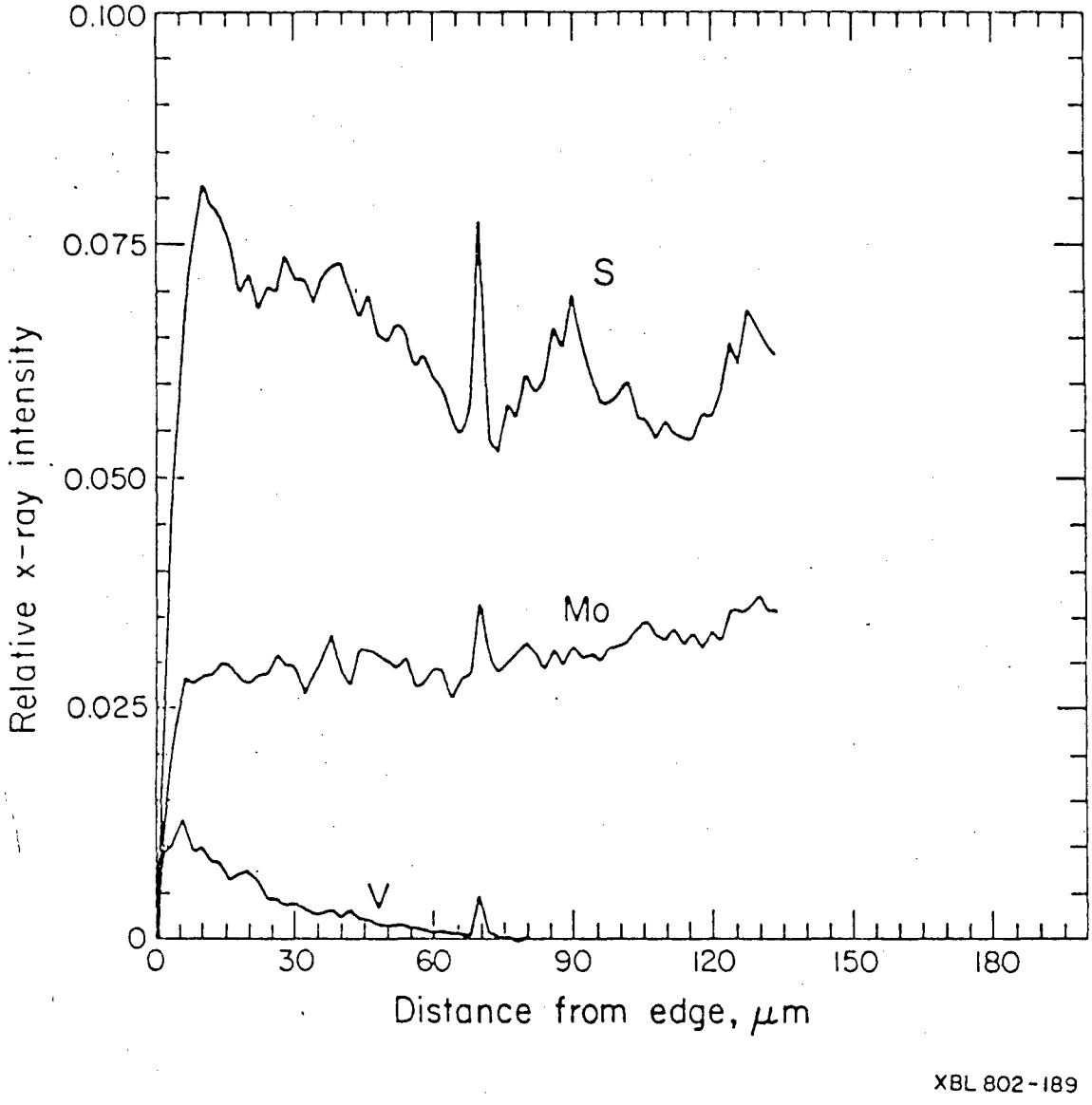
0.100
0.075
0.050
0.025
0
Relative x-ray intensity
S
Mo
V
0
30
60
90
120
150
180
Distance from edge, μm
XBL 802-189

Fig. 11

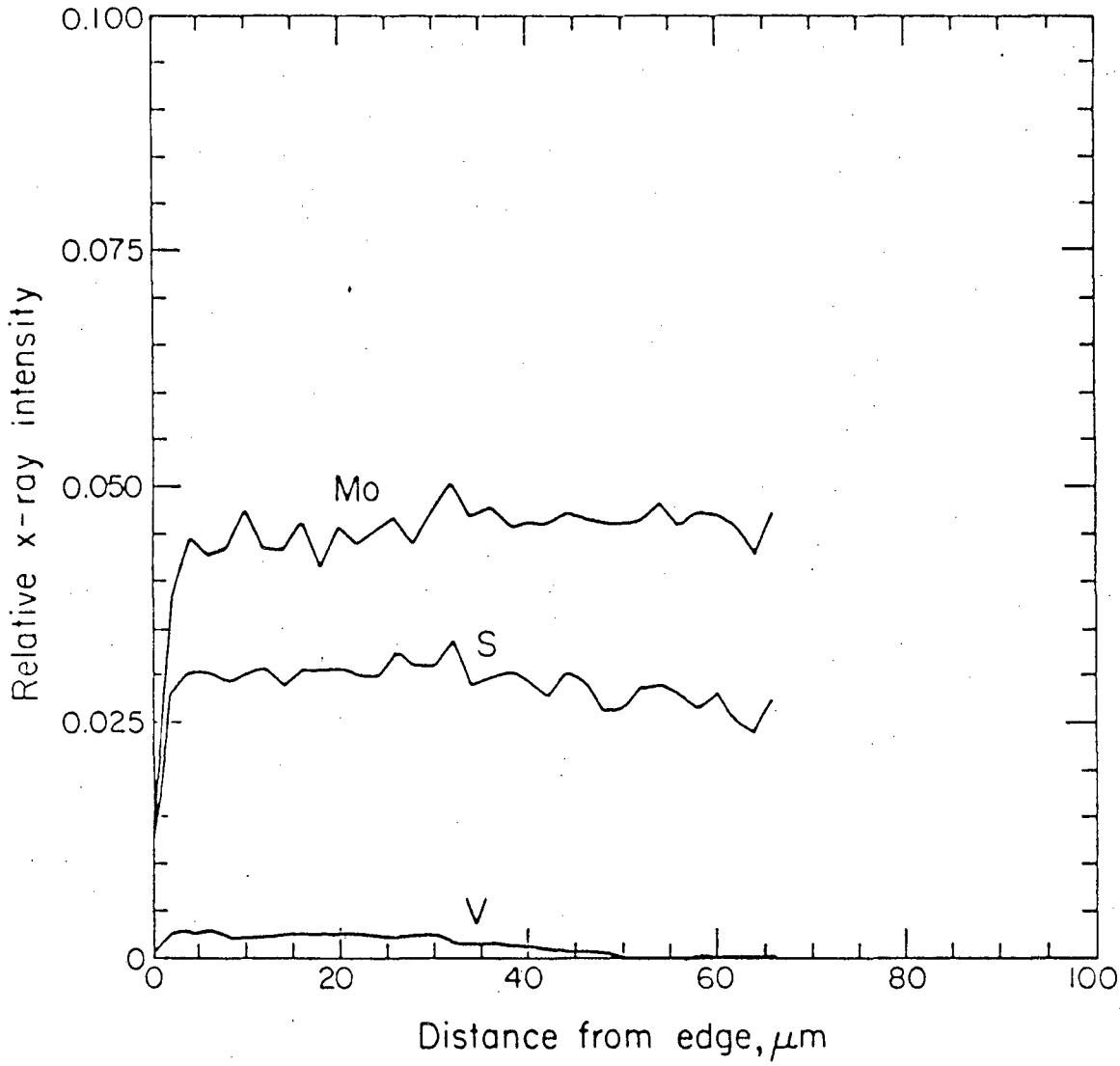

XBL 802-190

Fig. 12

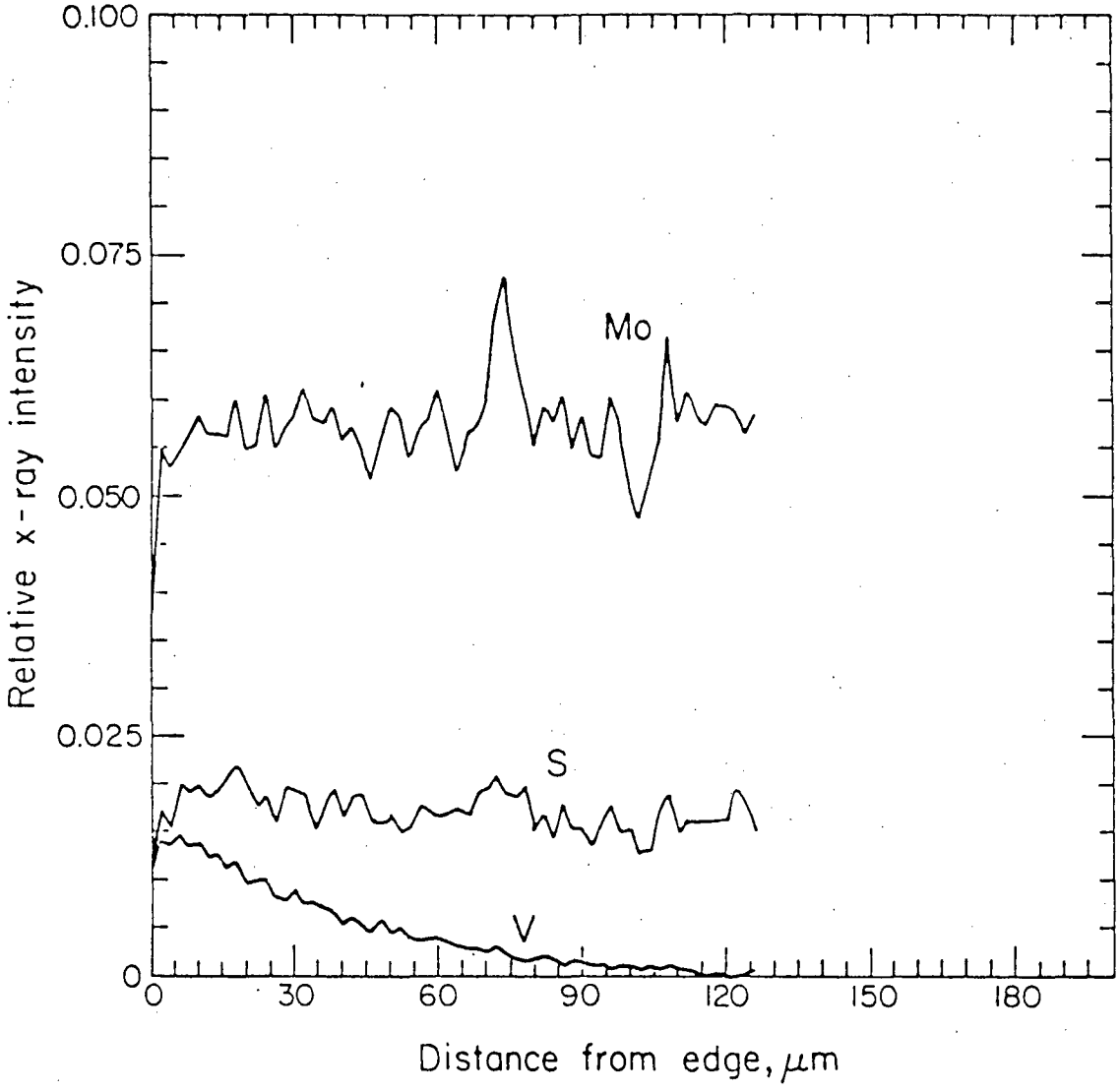

XBL 802-188

Fig. 13

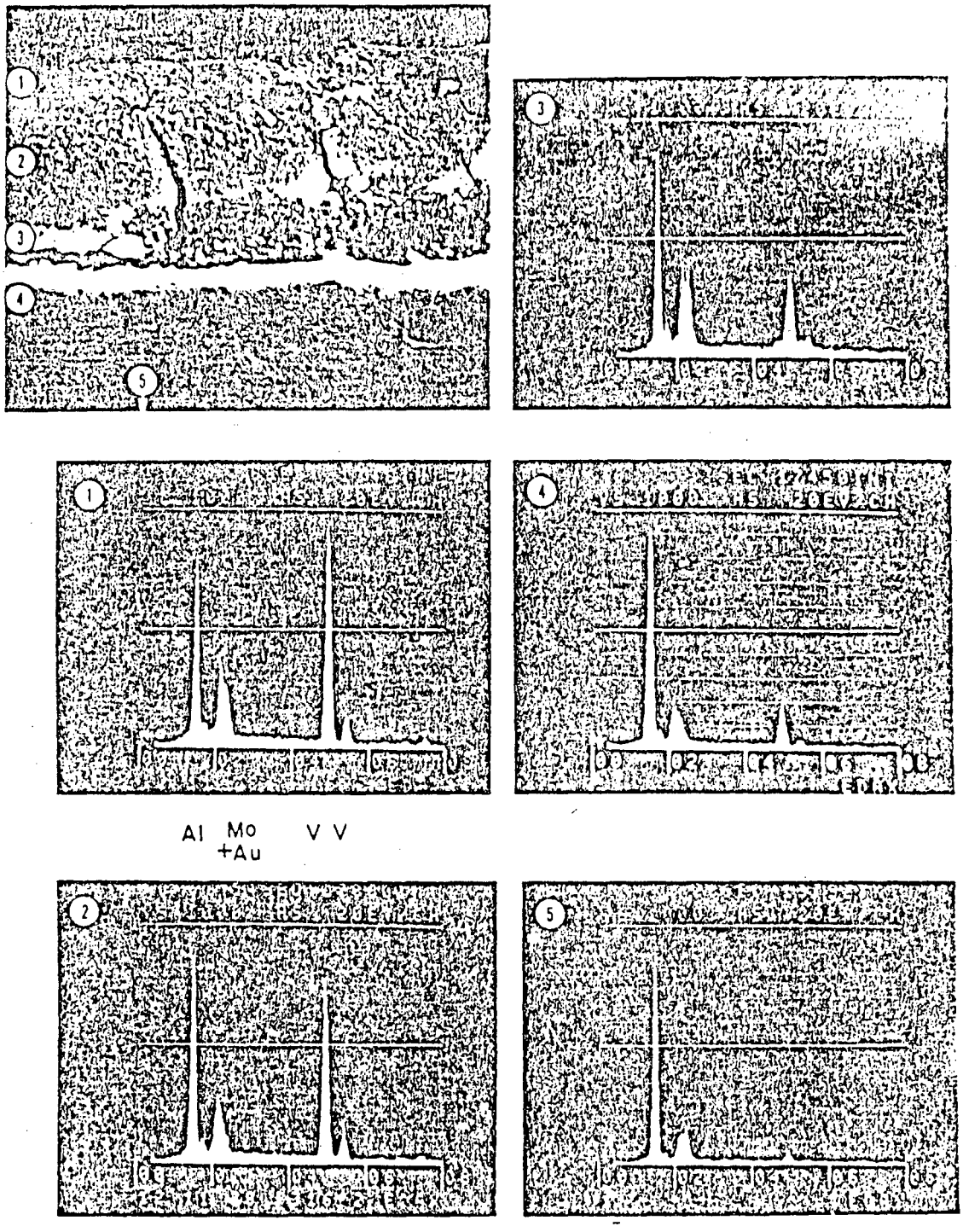

Fig. 14

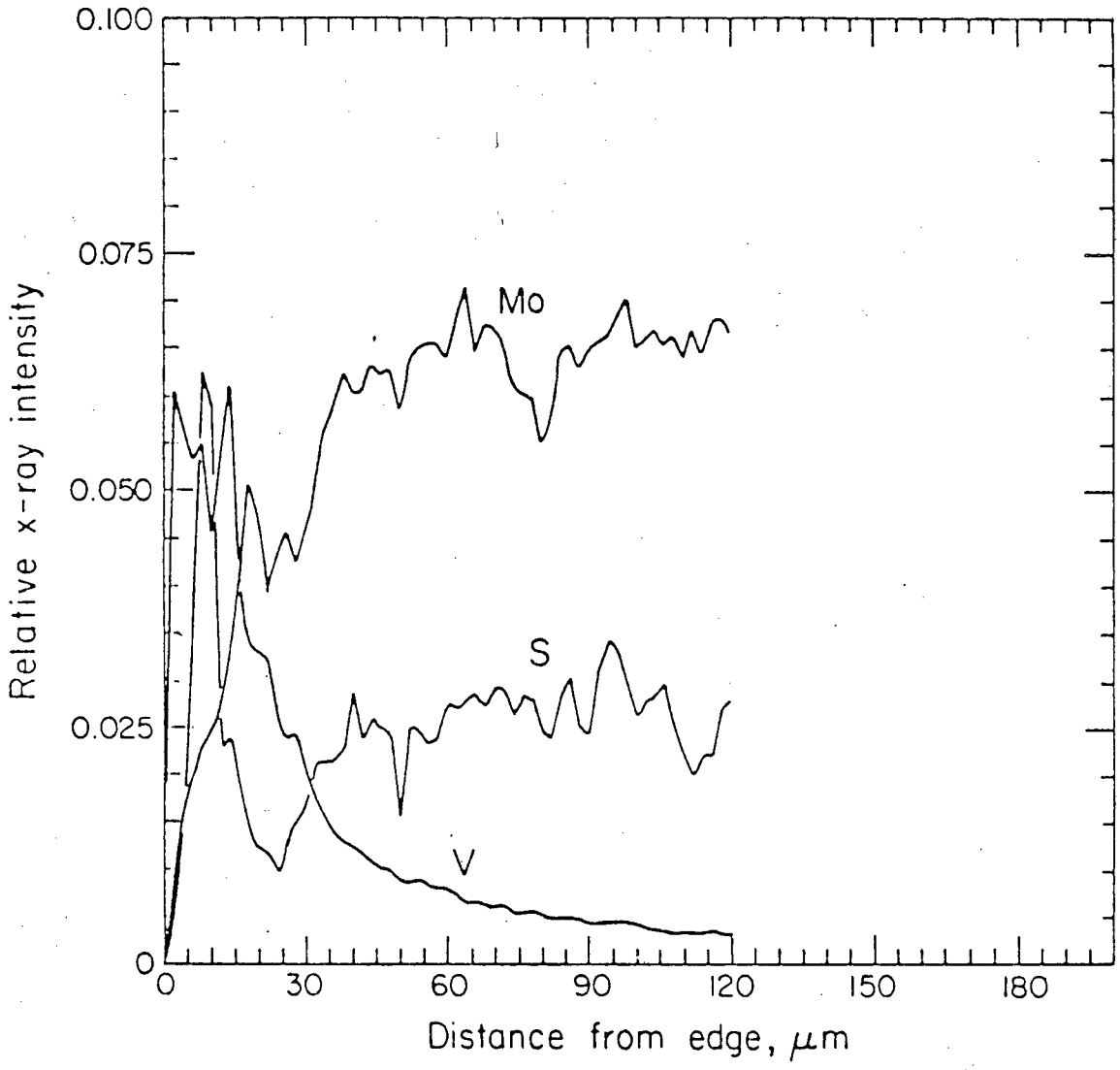
0.100
0.075
0.050
0.025
0
Relative x-ray intensity
Mo
S
V
0
30
60
90
120
150
180
Distance from edge, μm
XBL 802-187

Fig. 15

TECHNICAL INFORMATION DEPARTMENT
LAWRENCE BERKELEY LABORATORY
UNIVERSITY OF CALIFORNIA
BERKELEY, CALIFORNIA 94720